Hepatic differentiation of human pluripotent stem cells on human liver progenitor HepaRG-derived acellular matrix

Liisa K. Kanninen [a], Pauliina Porola [a], Johanna Niklander [a], Melina M. Malinen [a], Anne Corlu [b], Christiane Guguen-Guillouzo [b], Arto Urtti [a,c], Marjo L. Yliperttula [a], Yan-Ru Lou [a,*]

[a] Centre for Drug Research, Division of Pharmaceutical Biosciences, Faculty of Pharmacy, University of Helsinki, P.O. Box 56, FI-00014 Helsinki, Finland

[b] Inserm UMR991, Liver Metabolisms and cancer, Université de Rennes 1, F-35043 Rennes, France

[c] School of Pharmacy, University of Eastern Finland, P.O. Box 1627, 70211 Kuopio, Finland

* Corresponding author: Yan-Ru Lou. E-mail address: yan-ru.lou@helsinki.fi; Tel: +358 2941 59125; fax: +358 2941 59725

Running Title: HepaRG ACM for hepatic differentiation of hPSCs

Abstract

Human hepatocytes are extensively needed in drug discovery and development. Stem cell-derived hepatocytes are expected to be an improved and continuous model of human liver to study drug candidates. Generation of endoderm-derived hepatocytes from human pluripotent stem cells (hPSCs), including human embryonic stem cells and induced pluripotent stem cells, is a complex, challenging process requiring specific signals from soluble factors and insoluble matrices at each developmental stage. In this study, we used human liver progenitor HepaRG-derived acellular matrix (ACM) as a hepatic progenitor-specific matrix to induce hepatic commitment of hPSC-derived definitive endoderm (DE) cells. The DE cells showed much better attachment to the HepaRG ACM than other matrices tested and then differentiated towards hepatic cells, which expressed hepatocyte-specific makers. We demonstrate that Matrigel overlay induced hepatocyte phenotype and inhibited biliary epithelial differentiation in two hPSC lines studied. In conclusion, our study demonstrates that the HepaRG ACM, a hepatic progenitor-specific matrix, plays an important role in the hepatic differentiation of hPSCs.

Keywords

extracellular matrix; acellular matrix; human embryonic stem cell; human induced pluripotent stem cell; hepatic differentiation; HepaRG

1. Introduction

Human embryonic stem cells (hESCs) [1] and human induced pluripotent stem cells (hiPSCs) [2,3] have the ability to form all cell types of an adult body; thus they are highly interesting sources of cells for various human cell-based applications in the field of drug research. Hepatocytes are needed in drug discovery and development for prediction of biotransformation pathways, possible drug-drug interactions, and hepatotoxicity of a drug candidate. Differentiation of both hESCs and hiPSCs to hepatocyte-like cells has been studied broadly [4-8]; but still the biggest challenge is to obtain mature hepatocyte-like cells [9,10]. In the majority of the currently used differentiation protocols, stem cell fate is guided towards hepatocyte-like cells solely by a stepwise growth factor treatment. It is, however, known that not only soluble factors but also cell-cell interactions and cell-matrix interactions play an important role in the complex, multistage hepatic cell differentiation process [11].

Biomaterials mimicking the extracellular matrix (ECM) are ideal for *in vitro* cell culturing since they provide closely tissue-resembling microenvironments for cultured cells. ECM-mimicking *in vitro* culture systems can be established by using natural biomaterials, such as decellularized matrix, also called acellular matrix (ACM) [12] and ECM components, and synthetic biomaterials, such as synthetic polymeric hydrogels. Decellularized whole organs are the most natural, simulating scaffolds since tissue microarchitecture and its components such as proteins, glycosaminoglycans, and growth factors can be well maintained [13]. These scaffolds are useful in whole organ engineering [14], but due to demanding decellularization and repopulation processes using perfusion systems, they are not optimal matrices for *in vitro* high-throughput drug testing during drug development. In addition, whole organ ACM scaffolds cannot mimic a defined region of a tissue to induce cell type-specific effects.

During embryogenesis, the cells from definitive endoderm (DE) differentiate to a fully functional adult hepatocyte fate under specific matrices and hormonal conditions [15]. To mimic the *in vivo* differentiation process, *in vitro* hepatic differentiation most commonly starts from DE cells. The soluble factors used during *in vitro* hepatic differentiation have been given most of the focus of research efforts because they are available commercially in purified forms and can be easily added into culture media. Contrary, the optimal matrix for *in vitro* hepatic commitment of the DE cells is poorly understood, partially due to the complexity of matrix and unavailability of specific matrix components. Here we show that human liver progenitor cell-derived ACM supports the attachment of DE cells and their hepatic differentiation.

2. Materials and methods

2.1. *Preparation of the ACM*

We prepared the ACM from human liver progenitor HepaRG cells. The HepaRG cells [16] were obtained from Biopredic (Saint-Grégoire, France), and they were plated at 26,000 cells/cm^2 density and cultured for two weeks in previously prescribed culture conditions during which the cells are known to differentiate to hepatocyte-like cells and cholangiocyte-like cells through a bipotent progenitor [17,18]. Decellularization was performed as described earlier [19] with some modifications. The cell monolayer was first washed once with distilled water (Gibco, 15230-089) and then incubated with water for 45 minutes at 37°C. Next, the ACM was washed twice with water to ensure complete removal of the cells, and was used immediately for DE cell differentiation. The complete removal of HepaRG cells from the ACM using this protocol was confirmed by DAPI staining and Filamentous actin staining with Alexa Fluor 594 phalloidin (Invitrogen, A12381, 1:50) (data not shown).

2.2. Cell cultures

The hESC lines WA07 and H9 [1] and hiPSC line iPS(IMR90)-4 [3] were purchased from WiCell research institute. H9 cells were genetically modified to H9-GFP cells as described earlier by us [20].

Stem cells were maintained in standard Matrigel culture system (BD Biosciences, 356230, 0.5 mg per one 6-well plate) in mTeSR™1 medium (STEMCELL™ Technologies, 05850). The medium was changed daily. The WA07 and iPS(IMR90)-4 cells were passaged at a ratio of 1:5 every four days by using Versene 1:5000 (Invitrogen, 15040033). The H9-GFP cells were passaged at a ratio of 1:4-1:6 every four days by using Dispase (STEMCELL™ Technologies, 07923). Prior to cell passaging, differentiated cell areas were removed manually. All the cell cultures were maintained at 37°C in a humid atmosphere with 5% CO_2. The WA07, H9-GFP, and iPS(IMR90)-4 cells used in this study were at passages p38, p18(13)-p22(17), and p18+39(14), respectively.

HepaRG cells used as controls in qPCR were cultured for two or four weeks in the conditions described above. In the four-week culture, the medium was supplemented with 2% DMSO during the last two weeks to induce the maturation to hepatocyte-like cells.

2.3. Differentiation of the human pluripotent stem cells (hPSCs) to DE cells

Different induction medium compositions were tested to maximize the differentiation efficiency of the hPSCs to DE cells. RPMI-1640 medium (Gibco, 31870-025) was supplemented with four different sets of supplements (Fig. 1A). The selection of the supplements was based on earlier publications [21,22]. The media M1, M2, M3, and M4 were tested with the iPS(IMR90)-4 cells, media M2 and M4 with the WA07 cells, and medium M1 with the H9-GFP cells. The DE induction was performed for six days, and the media were renewed daily. The best medium was selected for each cell line for generating DE cells for the subsequent differentiation steps.

2.4. Hepatic differentiation of the DE cells

The DE cells were detached by a Cell Dissociation Buffer (Gibco, 13151-014) for 15 minutes at 37˚C followed by an Accutase cell detachment solution (Millipore, SCR005) for one to two minutes at room temperature. The hPSC-derived DE cells were seeded at a ratio of 1:1 onto the HepaRG-ACM. For comparison, we plated the DE cells on a standard cell culture dish, Matrigel-coated dish, rat

collagen type I-coated dish, mouse laminin-111-coated dish, or human collagen type III-coated dish. Matrigel coating was prepared according to the protocol used in the hPSC culture. A 12-well tissue culture plate was coated with collagen type I (Cultrex, 3440-100-01) at 50 µg/ml, laminin-111 (Cultrex, 3400-010-01) at 25 µg/ml, or collagen type III (Sigma, C4407) at 25 µg/ml for two hours at room temperature. Hepatic differentiation of the DE cells was induced in three steps. First, the cells were cultured in Hepatocyte Culture Medium (HCM™ SingleQuots™ Kit; Lonza CC-4182, without rhEGF and gentamicin-amphotericin-1000) supplemented with 5 ng/ml fibroblast growth factor 4 (FGF4, PeproTech, 100-31), 10 ng/ml bone morphogenetic protein 2 (BMP2, PeproTech, 120-02), and 10 ng/ml BMP4 (PeproTech, 120-05) for four days. Next, the cells were incubated in HCM supplemented with 10 ng/ml hepatocyte growth factor (HGF, PeproTech, 100-39), 10 ng/ml Oncostatin M (OSM, PeproTech , 300-10T), and 0.1 µM Dexamethasone (DEX, Sigma-Aldrich, D4902) for two to three days (WA07 and iPS(IMR90)-4) or four to six days (H9-GFP). Finally, the cells were cultured in HCM supplemented with 0.1 µM DEX for five days. Matrigel overlay was used in the last step of the differentiation. Briefly, the ice-cold Matrigel (BD Biosciences, 356230) was diluted into the medium at a concentration of 0.233 mg/ml and then added on top of the cells. After overnight incubation at 37°C, the Matrigel solution was gently replaced by the fresh medium.

2.5. Flow cytometry

The cells were detached by a Cell Dissociation Buffer and Accutase as described above. Single cell suspension was first incubated with mouse anti-stage-specific embryonic antigen-4 (*SSEA-4*, Developmental Studies Hybridoma Bank, MC-813-70, 1:400 in 2% FBS), rat anti-*SSEA-3* IgM (STEMCELL™ Technologies, 01553, 1:100 in 2% FBS), or mouse anti-chemokine receptor type 4 (*CXCR-4*, R&D Systems, MAB172, 1:50 in 2% FBS) on ice for 60 min. After washing, the cells were incubated with APC-conjugated goat anti-mouse IgG (H+L) (SouthernBiotech, 1031-11S, 1:300 in 2% FBS), APC-conjugated goat anti-rat IgM (STEMCELL™ Technologies, 10215, 1:100 in 2% FBS), or APC-conjugated goat anti-mouse IgG (H+L) (Beckman Coulter, 736830, 1:50 in 2% FBS)

on ice for 40 min in dark. The negative control sample was stained only with the secondary antibody. Cells were analyzed on a BD LSR II flow cytometer (633 nm laser, 660/20 BP filter detector) using BD FACSDiva software. The overlay histograms were created with Flowlogic software.

2.6. Immunostaining

For immunofluorescence cells were cultured in 8-well Lab-Tek® Chamber Slide™ systems (Nunc, 177445) or black 96-well µ-plates (ibidi, 89626). Cells were fixed with 4% paraformaldehyde for 10 minutes, permeabilized with 0.1% Triton X-100 or 0.5% Saponin for 10 minutes, and blocked with 10% normal goat or donkey serum (Millipore) for one hour. Cells were incubated with the primary antibodies (Table S1) overnight at +4°C. Negative controls were rabbit IgG (Santa Cruz Biotechnology, sc-2027), mouse IgG (Santa Cruz Biotechnology, sc-2025), and goat IgG (Santa Cruz Biotechnology, sc-2018). Next day the cells were incubated with the secondary antibody conjugated with Alexa Fluor 594 (Invitrogen, 1:400) for one hour. Filamentous actin was stained with Alexa Fluor 594 phalloidin (Invitrogen, A12381, 1:50). Nuclei were stained either with DAPI (Sigma-Aldrich, D8417, 25 µg/ml in MilliQ water) or with 0.2 µM SYTOX green (Invitrogen, S7020). The protein expression was visualized with a Leica TCS SP5II HCS A confocal microscope with an HCX PL APO 20x/0.7 Imm Cor (glycerol) objective. DAPI was excited with UV (diode 405 nm/50 mW), SYTOX green with an Argon 488 nm laser, and Alexa Fluor 594 with a DPSS (561 nm/20 mW) laser. The images were analyzed with Imaris 7.4 program (Bitplane) by creating slices or easy three-dimensional (3D) images. Immunofluorescence of the H9-GFP cells and their derivatives was imaged with a Zeiss Axioplan microscope.

2.7. RNA isolation, real-time qPCR, and analysis of the real-time qPCR data

Total RNA was extracted from the H9-GFP cells and their derivatives using a TRIzol reagent (Invitrogen, 15596) following the manufacturer's instructions. Other cells were lysed with a RLT-buffer (Qiagen), and total RNA was extracted using an RNeasy Mini kit (Qiagen, 74104) according to the manufacturer's instructions. Primary human hepatocytes (BD Biosciences, 454503, lot 95 and

lot 99) were used as controls. The frozen primary human hepatocytes were recovered by using a cryopreserved hepatocyte purification kit (BD Biosciences, 454500) according to the manufacturer's instructions. RNA concentrations were measured with a NanoDrop 2000 spectrophotometer (Thermo Fischer Scientific). The RNA was converted to cDNA with a High Capacity RNA-to-cDNA kit (Applied Biosystems, 4387406). The cDNA samples (10 ng in 20 µl reaction) were analyzed in duplicate on a StepOnePlus Real-Time PCR System (Applied Biosystems) using a Fast SYBR Green Master Mix (Applied Biosystems, 4385612). Housekeeping gene ribosomal protein, large, P0 (*RPLP0*) served as an endogenous control. PCR cycles were as follows: 40 cycles at 95°C for 3 s and annealing/extension at 60°C for 30 s. The primers were designed by Primer Express v2.0 software (Applied Biosystems) except the primers for *OCT4* [3] and *HNF3B* [21]. All the primers were synthesized by Oligomer Oy (Helsinki, Finland), and their sequences are shown in Table S2. A standard curve for each gene was generated, and the amplification efficiency was used in calculating the relative quantification of the target gene in comparison to the housekeeping gene with an earlier described mathematical model [23].

2.8. ALB secretion and total protein analysis

The hepatic functions of the derived cells were analyzed by determining the secreted *ALB*. Cell culture media were collected 24 h after medium renewal and frozen for later analysis. Each collected medium sample was analyzed in duplicate with a Human Albumin ELISA kit (Bethyl Laboratories) following the manufacturer's instructions. The secreted *ALB* amount was calculated with a standard curve and normalized with the total cellular protein amount. The cellular protein samples were prepared as follows: cells were lysed with a RIPA buffer (Pierce Biotechnology), and the total protein amount was quantified with a BCA Protein Assay kit (Pierce Biotechnology) according to the manufacturer's instructions.

3. Results

3.1. Characterization of the hPSCs

Before differentiating the hPSCs towards DE cells, we checked their pluripotency. Immunofluorescence of the key pluripotent markers showed that the WA07 and iPS(IMR90)-4 cells highly expressed the transcription factor *OCT4* and the surface marker *SSEA-4* and that the H9-GFP cells highly expressed *OCT4* (Fig. S1A). In addition, flow cytometry showed that 99.7% of the WA07 cells and 93.5% of the iPS(IMR90)-4 cells were positive for *SSEA-4* and that 95.3% of the H9-GFP cells were positive for *SSEA-3* (Fig. S1B). The H9-GFP, WA07, and iPS(IMR90)-4 cells did not express the hepatic differentiation markers *AFP* and *HNF4A* (Fig. S2A).

3.2. Differentiation of the hPSCs to DE cells

We first differentiated the H9-GFP cells to DE cells in the medium M1 (Fig. 1A) according to a published protocol [24]. After six days in the medium M1, the cells showed uniform morphology (Fig. 1E). The majority of the derived cells were positive for the DE markers *HNF3B* and *CXCR-4* (Fig. 2), and 95.7% of them expressed *CXCR-4* (Fig. 1F). When using the same medium M1 for the WA07 and iPS(IMR90)-4 cells, a pure cell population with DE morphology was produced already in the first one to two days followed by a massive cell death (Fig. 1B). The derived DE cells continued dying in the medium M1, and therefore the yield was very low. To optimize the induction medium used to differentiate the WA07 and iPS(IMR90)-4 cells to DE cells, we tested four different media (Fig. 1A). The media containing Activin A and B-27 (M2 and M4) yielded much more DE cells compared with the media containing also Wnt-3a and sodium butyrate (M1 and M3). Indeed, after two days of the induction, the iPS(IMR90)-4-derived DE cells in the Wnt-3a and sodium butyrate supplemented media were severely suffering (Fig. 1B). Due to the low yield of DE cells, we did not continue these cultures any longer. We also tested two Activin A products. We did not notice remarkable difference in the phenotype of the WA07 or iPS(IMR90)-4-derived DE cells between two Activin A products as the cell morphology, cell density, and *CXCR-4* expression in the hPSC-derived DE cells were similar (Fig. 1C, 1D and 1F). The medium M2 was chosen for generating DE cells from the WA07 and iPS(IMR90)-4 cells for the following differentiation to hepatic lineage.

After six days of DE induction, the majority of the WA07 and iPS(IMR90)-4-derived cells expressed *HNF3B* and *CXCR-4* proteins (Fig. 2), but not *AFP* or *HNF4A* proteins (Fig. S2B). Flow cytometry revealed that 93.8% of the WA07-derived DE cells and 82% of the iPS(IMR90)-4-derived DE cells were positive for *CXCR-4* (Fig. 1F).

3.3. Hepatic differentiation of the hPSC-derived DE cells

The DE cells were differentiated towards hepatic cells with a three-step differentiation protocol, namely hepatic commitment, hepatic progenitor expansion, and hepatic maturation (Fig. 3A). The DE cells were produced in a Matrigel-coated dish where the hPSCs were cultured. As Matrigel may not be an ideal matrix for hepatic commitment of the DE cells, we tested different matrices for the attachment of the hPSC-derived DE cells. Only a few DE cells attached to the standard cell culture dish, Matrigel-coated dish, rat collagen type I-coated dish, and mouse laminin-111-coated dish (Fig. S3), and none attached to human collagen type III-coated dish (data not shown). Therefore, these cultures were stopped after two days. In contrast, the DE cells well attached to the HepaRG-derived ACM (Fig. S3). We then induced hepatic commitment in this condition using BMP2, BMP4, and FGF4. The H9-GFP, WA07, and iPS(IRM90)-4-derived DE cells formed confluent monolayer on the HepaRG-ACM after four-day treatment (Day 10, Fig. 3B). The cells showed polygonal-shaped morphology with cytoplasmic vacuoles and pericytoplasmic actin as seen under a phase contrast microscopy and by F-actin staining, respectively (Fig. 3B and 3C). Some of the cells were binucleated. These morphological characteristics were previously reported for hESC-derived hepatocytes [6,25] and were similar to cultured human primary hepatocytes [26-28]. The H9-GFP-derived cells formed homogenous monolayer by day 18 (Fig. 3B). The expression of hepatic progenitor markers was studied by immunofluorescence. The WA07, iPS(IMR90)-4, and H9-GFP-derived progenitors expressed *HNF4A* and *CK-19* proteins (Fig. 4A), but they were negative for *AFP* on day 10 (data not shown). The protein expression level seems to vary among the cells in the same

culture, particularly in the H9-GFP cells. The WA07-derived cells showed the highest expression level of *HNF4A* protein among the three cell lines. The *AFP* protein expression appeared later, on day 13 in the WA07 and iPS(IMR90)-4-derived progenitors and on day 14 in the H9-GFP-derived progenitors (Fig. 4B).

In the next differentiation steps, the hepatic progenitors were expanded in the presence of HGF, OSM, and DEX, after which hepatic maturation was induced by DEX. Matrigel overlay was tested during the maturation. The expression of hepatic markers was studied at protein level. On day 18, the WA07-derived hepatic cells were highly positive for *HNF4A* and partially positive for *ALB*, *CYP3A4*, and *AFP* shown by immunofluorescence (Fig. 5). The iPS(IMR90)-4-derived cells were weakly positive for *HNF4A* and *CYP3A4*, and negative for *ALB*. The minority of the iPS(IMR90)-4-derived cells were positive for *AFP*. The majority of the H9-GFP-derived hepatic cells were positive for *HNF4A* and partially positive for *ALB* and *AFP* (Fig. 5). In our preliminary tests, we observed cell migration and formation of ductular structures that eventually detached from the culture dish in the presence of HGF in the hepatic maturation step (Fig. S4). When HGF was omitted and Matrigel overlay was applied, the formation of ductular structures was prevented. Matrigel overlay showed little effect on the protein expression of the studied markers in the WA07 and iPS(IMR90)-4 cells, but it decreased the *AFP* protein expression and induced the expression of a hepatic transporter protein, *MRP2*, in the H9-GFP-derived hepatic cells on day 19 (Fig. 5). Without Matrigel overlay, the *MRP2* protein was not detected in the H9-GFP-derived hepatic cells on days 14, 16, and 21 (data not shown).

Hepatic functions of the H9-GFP-derived cells were investigated by measuring *ALB* secretion. From day 16 to day 21, the hepatic cells increased their *ALB* protein production, and on the last time point, the cells secreted 119 ng *ALB* per mg total cellular proteins per day (Fig. S5).

3.4. Gene expression profiles in the hPSCs and their derivatives during differentiation

We studied the transcriptional profiles of pluripotency and liver specific genes in the three cell lines during the differentiation and also compared the levels with those in the human primary hepatocytes, HepaRG, and HepG2 cells by qPCR. The mRNA expression levels of the pluripotency markers *OCT4* (Fig. 6) and *NANOG* (Fig. S6) in the WA07 and iPS(IMR90)-4-derived cells decreased to the levels similar to those in the human primary hepatocytes and HepaRG cells as shown by qPCR. The mRNA expression of *HNF3B* (*FOXA2*), a maker of foregut endoderm [29], increased about 200-250-fold in the DE cells (day 6) and hepatic progenitor cells (day 10) and then dropped to the level similar to that in the HepaRG cells, which was much lower than that in the human primary hepatocytes (Fig. 6). The mRNA expression of the liver specific cytokeratins *CK-8* and *CK-18* increased to the maximal levels at day 12 and then decreased at day 17 in the WA07 and iPS(IMR90)-4-derived cells (Fig. 6). In the H9-GFP cells, the mRNA expression of *CK-8* and *CK-18* was constantly increasing during differentiation (Fig. S7). The WA07, iPS(IMR90)-4, and H9-GFP-derived cells still expressed *AFP* and *CK-19* in the final studied time point, which indicates that the cells were not mature hepatocytes yet (Fig. 6 and S7). The expression of the hepatocyte markers *ALB* and alpha-1 antitrypsin (*AAT*) was increasing during the culture period confirming the hepatic lineage differentiation, but the expression level was much lower than the levels in the human primary hepatocytes, HepaRG cells, or HepG2 cells (Fig. 6 and S7).

Matrigel overlay greatly increased the mRNA expression of *ALB* and *AAT* and slightly decreased the mRNA expression of *CK-19* in the WA07-derived hepatic cells compared with the cells without Matrigel overlay, but it did not affect the expression of *AFP* (Fig. 6A). On the other hand, the expression of *APF*, *ALB*, and *AAT* in the iPS(IMR90)-4-derived cells was decreased in the presence of Matrigel overlay (Fig. 6B).

We were interested to know how the markers of hepatic stem cells and hepatoblasts changed during the differentiation. Neural cell adhesion molecule 1 (*NCAM1*), a marker of hepatic stem cells [30], was expressed at a very low level in the human primary hepatocytes but at much higher levels in the WA07 and iPS(IMR90)-4-derived hepatic cells and HepaRG cells (Fig. S6). Intercellular adhesion molecule 1 (*ICAM1*), a marker of hepatoblasts [30], was expressed at lower levels in the WA07 and iPS(IMR90)-4-derived hepatic cells than in the human primary hepatocytes and HepaRG cells (Fig. S6).

The mRNA expression of ATP-binding cassette, sub-family B, member 1 (*MDR1*, *ABCB1*), one of the important drug transporters, in the H9-GFP cells was increased during the differentiation (Fig. S7), but the level was still lower than those in the HepaRG and HepG2 cells.

We also noticed that HepaRG cells expressed a hepatoblast marker, *CK-19*, which was slightly increased by the 2-week treatment with 2% DMSO (Fig. 6). The mRNA expression levels of *CK-8* and *CK-18* in the 2-week cultured HepaRG cells was similar to that in the undifferentiated stem cells, but was increased by the 2-week treatment with 2% DMSO (Fig. 6). This confirms that the HepaRG cells used to produce the ACM were at the progenitor stage.

4. Discussion

Human PSCs offer a great supply of all types of somatic cells for basic research and biomedical applications, and thus the *in vitro* differentiation has been extensively studied. Generation of DE-derived hepatocytes from hPSCs is a complex, challenging process requiring specific signals from soluble factors and insoluble matrices at each developmental stage. In the present study, we exploited the use of HepaRG-derived ACM in hepatic differentiation of hPSCs and found that the HepaRG-ACM supported the attachment of hPSC-derived DE cells and their differentiation towards hepatic cells.

4.1. The role of the ECM in hepatic commitment of DE cells

The ECM is dynamic, and its remodeling is an important mechanism by which cell differentiation and tissue formation are regulated [31,32]. To induce hepatic commitment, most attention and effort have been paid to the selection of soluble factors, but not to the compositions of matrices. Little is known about the exact matrix environments for DE induction and hepatic commitment. Researchers have used the same matrices for both DE induction of hPSCs and hepatic commitment of DE cells, such as feeder cells [4,6] or Matrigel [7], which are used for the culture of hPSCs. We hypothesized that the ACM derived from the human liver progenitor HepaRG cells would provide the environment for the hepatic commitment of hPSC-derived DE cells. The HepaRG-derived ACM represents a hepatic progenitor-specific matrix for DE cells because the next step in the hepatic differentiation process for DE cells is hepatic progenitor. We observed good attachment of the DE cells on the HepaRG-ACM. In contrast, we saw a poor or lack of the DE cell attachment to the standard cell culture dish, Matrigel-coated dish, collagen type I-coated dish, laminin 111-coated dish, and collagen III-coated dish. The hESC-derived DE cells have earlier been reported to attach to collagen type I [5,6]. To select the optimal matrix components for hESCs and DE cells, researchers have focused on the expression of integrins. An earlier study revealed that a set of six integrins were upregulated in hESC-derived DE cells and that fibronectin and vitronection promoted efficient pancreatic differentiation of DE cells [33]. Another study described the finding of integrins αV and β5 on DE cells and suggested that vitronectin would be a suitable matrix [34]. Many integrins can bind to more than one ligand. For example, integrins αV and β5 can bind not only to vitronectin, but also to bone sialoprotein and osteopontin [35]. Cells may express more than one pair of integrins, as described earlier [33]. Thus, studying the expression of integrins makes it less efficient to screen for the optimal matrices. In contrast, our approach was to provide the liver progenitor environment to DE cells in order to induce hepatic commitment. Plating DE cells to a suitable environment also purifies the cell population and removes unwanted cell types. The characterization of the HepaRG-ACM is under

investigation in our laboratory, and it will guide us to produce fully synthetic matrix without human-derived components.

Acellular matrices are attractive *in vitro* culture scaffolds offering close mimics of *in vivo* cellular microenvironment since the physical structure together with biochemical components can be well-preserved after decellularization process [36]. Whole livers [36], liver slices [37], and cultured liver cells [19] have been used to produce ACM. Decellularized whole organs are suitable in the near future for organ transplantation [38]; however, the complex decellularization process of whole organs and the variability between organs hinder their use in industrial scales, particularly in drug testing applications. On the other hand, the decellularization of cultured cells can be performed without sophisticated equipment. In addition, cell-derived ACM can exert cell type-specific effect. Cultured cell-derived ACM has been used in directing the differentiation of ESCs to pancreatic cells [39] and the osteogenesis [40], adipogenesis [41], and chondrogenesis [42] of mesenchymal stem cells (MSCs). The fetal MSC-derived ACM was shown to enhance the *ex vivo* expansion of adult MSCs [43].

4.2. DE differentiation conditions vary between hPSC lines

DE-like cells have been generated from hPSCs in feeder-free culture without serum using various combinations of the following components: Activin A [21], B-27 [22], Wnt-3a and sodium butyrate [7,24], insulin-transferrin-selenium, and albumin [4]. We used different DE induction media for the H9-GFP cells than for the WA07 and iPS(IMR90)-4 cells since we noticed that the media supplemented with Wnt-3a and sodium butyrate reduced cell viability. Thus, the optimization of DE induction step is crucial, and in our experience it is needed for every hPSC line. Although different DE induction media were used, the expression of the DE markers *CXCR-4* and *HNF3B* was increased to a similar extent in all the studied cell lines after six days of induction. We obtained about 82-96% *CXCR-4* positive cells and more than 90% *HNF3B* positive cells from all three cell lines at this stage.

The reason for such difference in DE induction conditions between cell lines is unknown and is currently under investigation in our laboratory. Sodium butyrate is a known inhibitor of histone deacetylase [44], and at the concentration of 0.5 mM and above, it can cause cell differentiation followed by cell death [45]. Considerable cell death in the DE induction of hESCs was reported earlier [46].

4.3. Differentiation capacity varies between hPSC lines

In this study, we have found that different hPSC lines responded differently to the hepatic differentiation conditions. Before hepatic differentiation, the DE cells derived from all three cell lines expressed *CXCR-4* and *HNF3B* at similar levels. Immunofluorescence showed that more than 90% of the DE cells were positive for *HNF3B*, indicating that the cells from all three cell lines should be competent to commit to hepatic lineage because *HNF3B* plays a critical role in the initiation of early liver development [29] but is not important in maintenance of liver functions in adult hepatocytes [47]. Immunostaining of the lineage markers suggests that the WA07 cells have the best hepatic differentiation capacity among all three cell lines tested. More than 90% of the WA07 cells on day 10 and H9-GFP cells on day 16 were positive for *HNF4A*; however, this was not the case for the iPS(IMR90)-4 cells. The study on mouse embryonic development demonstrated the critical role of *HNF4A* in functional liver development [48]. The low expression level of *HNF4A* in the iPS(IMR90)-4-derived cells may explain the failure of the hepatic differentiation.

The variability of hepatic differentiation between hPSC lines has been noted before. An earlier study compared 28 hiPSC lines and found that hiPSCs derived from adult fibroblasts differentiated poorly, which was attributable to donor differences [49]. Variations have also been observed in neural differentiation [50] and endothelial differentiation [51] of different hPSC lines.

4.4. Maturation of hPSC-derived hepatic cells remains a challenge

Adult, mature hepatocytes have not so far been generated from hPSCs [9,10]. The phenotype of hPSC-derived hepatic cells closely resembles a fetal, immature hepatocyte phenotype [9,10]. All the hepatocyte-like cells derived from hPSCs reported earlier were *AFP* positive [4,6,7,22,24,49]. Ogawa, et al. successfully decreased the number of *AFP* positive cells to 34% by using cyclic adenosine monophosphate in aggregate culture [52]. In this study, we attempted to improve hepatic maturation by using several methods. HGF can induce the proliferation of hepatocytes but also their transdifferentiation to biliary epithelia [53,54]. Therefore, we used HGF during the hepatic expansion step and then removed it from the hepatic maturation step. Additionally, we applied Matrigel overlay in the hepatic maturation step because Matrigel overlay was earlier shown to inhibit biliary epithelial differentiation of primary mature adult hepatocytes and induce a mature hepatocyte phenotype [53]. In our preliminary tests, we observed cell migration and eventually the formation of ductular structures similar to bile ductules in the presence of HGF in the hepatic maturation step. This phenomenon has also been observed in primary hepatocyte culture [53]. When we omitted HGF and applied Matrigel overlay in the hepatic maturation step, we were able to prevent the formation of the ductular structures. In addition, we found that Matrigel overlay enhanced hepatocyte phenotype, evidenced by the increased expression of *ALB* and *AAT* in the WA07 cells, decreased expression of *CK19* in the WA07 cells, increased expression of *MRP2* in the H9-GFP cells, and decreased expression of *AFP* in the H9-GFP cells. The reason why Matrigel overlay did not produce the expected effect on the iPS(IMR90)-4-derived cells might be that the cells under Matrigel overlay were phenotypically different from those derived from the WA07 and H9-GFP cells, as seen from the immunofluorescence of the lineage markers. Since the derived cells from all three hPSC lines were still positive for the immature marker *AFP* except the H9-GFP-derived cells under Matrigel overlay, we did not measure mature liver functions related to drug metabolism and transport.

To promote hepatic maturation, the optimal matrices should be used together with soluble factors, which can maintain hepatocyte phenotype and inhibit biliary epithelial differentiation. The knowledge obtained from primary hepatocyte cultures can be utilized in the hepatic maturation step of hPSC differentiation. Various culture systems have been developed to maintain and enhance liver functions of primary hepatocytes. Sandwich culture [55], 3D scaffolds [56], and microcapsules [57,58] have been used successfully to enhance liver functions of primary hepatocytes. In addition, in view of our findings mentioned above and also in view of other findings about the role of ACM in directing stem cell fate, reviewed by Hoshiba, et al [13], a complete *in vitro* hepatic maturation may require a specific matrix environment.

5. Conclusions

The ECM and ECM-mimicking biomaterials have recently been shown to be important in controlling stem cell fate. The ECM is dynamic, and its remodeling is an important mechanism by which cell differentiation and tissue formation are regulated. For *in vitro* stem cell differentiation, the dynamic feature of the ECM must be understood to produce desired cell phenotypes. This study shows that the human liver progenitor HepaRG-derived ACM promotes the hepatic commitment and further differentiation of the hPSC-derived DE cells. Our study sheds light on the important role of the ECM in directing stem cell fate and provides new approaches to the improvement of hepatic maturation.

Author contributions

Y.-R.L. conceived and designed the study; L.K.K., P.P., J.N., and Y.-R.L. carried out the experiments; M.M.M. advised the culture of HepaRG cells; A.C. and C.G.-G. provided HepaRG cells; L.K.K and Y.-R.L. analyzed the data; M.L.Y. and A.U. commented on the research; Y.-R.L. and L.K.K. wrote the paper; all the authors commented on the final version of the paper.

Acknowledgments

This work was supported by EU-FP7 (LIV-ES project, HEALTH-F5-2008-223317), BioCenter Finland, Academy of Finland, and Tekes-The Finnish Funding Agency for Technology and

Innovation. L.K.K. acknowledges the Doctoral Programme in Materials Research and Nanosciences and the National Doctoral Programme in Nanoscience. Y.-R.L. acknowledges support from the Academy of Finland (No. 294193 and No. 294194). The authors would like to thank Dr. Kimmo Tanhuanpää and Mr. Mika Molin from the Light Microscopy Unit, Institute of Biotechnology for the guidance in confocal microscopy and image analysis, Ms. Maria Aatonen and Ms. Maria Semenova from the Department of Biosciences, Faculty of Biological and Environmental Sciences, University of Helsinki for their help with flow cytometry analysis, and Drs. Luke A. Noon and Deborah Burks from Principe Felipe Centro de Investigacion, Spain for providing the H9-GFP cells.

Supporting information

Supplementary data associated with this article includes seven figures and two tables and can be found in the online version.

Figure Legends

Fig. 1. Optimization of the medium components for the DE induction. (A) The reagents used to supplement RPMI-1640 medium for the DE induction media M1, M2, M3, and M4. (B) The iPS(IMR90)-4 cells in the DE induction media on day 2. (C) The iPS(IMR90)-4 cells after 6 days in the M2 and M4 media. (D) The WA07 cells after 6 days in the M2 and M4 media. (E) The H9-GFP cells after 6 days in the M1 medium. Scale bars = 100 µm. (F) Flow cytometry analysis of the *CXCR-4* expression in the WA07 and iPS(IMR90)-4-derived cells after 6 days in the media M2 and M4 and H9-GFP-derived cells after 6 days in the medium M1.

Fig. 2. Characterization of the hPSC-derived DE cells. Immunofluorescence of *HNF3B* and *CXCR-4*. Scale bars = 100 µm. 20x magnification for the H9-GFP cells.

Fig. 3. Hepatic differentiation of the hPSC-derived DE cells in the HepaRG-derived ACM system. (A) A stepwise differentiation process. (B) Phase contrast microscope images of the cells at different time points. **(**C) Filamentous actin (F-actin) staining shows polygonal-shaped morphology of the iPS(IMR90)-4-derived cells. F-actin = red, nuclei = blue. MO = Matrigel overlay. Scale bars = 100 µm.

Fig. 4. Immunostaining of the liver markers in the cells differentiated on the HepaRG-derived ACM. (A) The cells on day 10. (B) The WA07 and iPS(IMR90)-4 cells on day 13 and H9-GFP cells on day 14. Scale bars = 100 µm. 10x magnification for the H9-GFP cells.

Fig. 5. Effect of Matrigel overlay (MO) on hepatic maturation. Immunostaining of the liver markers in the WA07 and iPS(IMR90)-4 cells on day 18 and in the H9-GFP cells on day 16 and day 19 (+ MO). Scale bars = 100 µm. 10x magnification for the H9-GFP cells.

Fig. 6. Relative mRNA expression of the pluripotency and liver markers in the WA07 and iPS(IMR90)-4 cells during the differentiation. The mRNA expression of *OCT4*, *HNF3B*, *AFP*, *CK-19*, *CK-18*, *CK-8*, *ALB*, and *AAT* in the WA07 (A) and iPS(IMR90)-4 (B) cells during the differentiation was analyzed by real-time qPCR. Relative mRNA expression was normalized to the

control gene *RPLP0*, and fold inductions were calculated with reference to the undifferentiated WA07 or iPS(IMR90)-4 cells on day 0. N = 3 biological samples. Error bars are SD. MO = Matrigel overlay; PHH 1: primary human hepatocytes (BD Biosciences, 454503, lot 95); PHH 2: primary human hepatocytes (BD Biosciences, 454503, lot 99); HepaRG 1: two-week culture without DMSO treatment; HepaRG 2: two-week culture without DMSO treatment followed by two week differentiation in 2% DMSO.

References

[1] J.A. Thomson, J. Itskovitz-Eldor, S.S. Shapiro, M.A. Waknitz, J.J. Swiergiel, V.S. Marshall, J.M. Jones, Embryonic stem cell lines derived from human blastocysts, Science 282 (1998) 1145-1147.
[2] K. Takahashi, K. Tanabe, M. Ohnuki, M. Narita, T. Ichisaka, K. Tomoda, S. Yamanaka, Induction of pluripotent stem cells from adult human fibroblasts by defined factors, Cell 131 (2007) 861-872.
[3] J. Yu, M.A. Vodyanik, K. Smuga-Otto, J. Antosiewicz-Bourget, J.L. Frane, S. Tian, J. Nie, G.A. Jonsdottir, V. Ruotti, R. Stewart, Slukvin, II, J.A. Thomson, Induced pluripotent stem cell lines derived from human somatic cells, Science 318 (2007) 1917-1920.
[4] J. Cai, Y. Zhao, Y. Liu, F. Ye, Z. Song, H. Qin, S. Meng, Y. Chen, R. Zhou, X. Song, Y. Guo, M. Ding, H. Deng, Directed differentiation of human embryonic stem cells into functional hepatic cells, Hepatology 45 (2007) 1229-1239.
[5] Y. Duan, X. Ma, W. Zou, C. Wang, I.S. Bahbahan, T.P. Ahuja, V. Tolstikov, M.A. Zern, Differentiation and characterization of metabolically functioning hepatocytes from human embryonic stem cells, Stem Cells 28 (2010) 674-686.
[6] S. Agarwal, K.L. Holton, R. Lanza, Efficient differentiation of functional hepatocytes from human embryonic stem cells, Stem Cells 26 (2008) 1117-1127.
[7] D.C. Hay, D. Zhao, J. Fletcher, Z.A. Hewitt, D. McLean, A. Urruticoechea-Uriguen, J.R. Black, C. Elcombe, J.A. Ross, R. Wolf, W. Cui, Efficient differentiation of hepatocytes from human embryonic stem cells exhibiting markers recapitulating liver development in vivo, Stem Cells 26 (2008) 894-902.
[8] K. Si-Tayeb, F.K. Noto, M. Nagaoka, J. Li, M.A. Battle, C. Duris, P.E. North, S. Dalton, S.A. Duncan, Highly efficient generation of human hepatocyte-like cells from induced pluripotent stem cells, Hepatology 51 (2010) 297-305.
[9] R.E. Schwartz, H.E. Fleming, S.R. Khetani, S.N. Bhatia, Pluripotent stem cell-derived hepatocyte-like cells, Biotechnol Adv 32 (2014) 504-513.
[10] M. Baxter, S. Withey, S. Harrison, C.P. Segeritz, F. Zhang, R. Atkinson-Dell, C. Rowe, D.T. Gerrard, R. Sison-Young, R. Jenkins, J. Henry, A.A. Berry, L. Mohamet, M. Best, S.W. Fenwick, H. Malik, N.R. Kitteringham, C.E. Goldring, K. Piper Hanley, L. Vallier, N.A. Hanley, Phenotypic and functional analyses show stem cell-derived hepatocyte-like cells better mimic fetal rather than adult hepatocytes, J Hepatol 62 (2015) 581-589.
[11] C.M. DiPersio, D.A. Jackson, K.S. Zaret, The extracellular matrix coordinately modulates liver transcription factors and hepatocyte morphology, Mol Cell Biol 11 (1991) 4405-4414.
[12] S.F. Badylak, The extracellular matrix as a biologic scaffold material, Biomaterials 28 (2007) 3587-3593.
[13] T. Hoshiba, H. Lu, N. Kawazoe, G. Chen, Decellularized matrices for tissue engineering, Expert Opin Biol Ther 10 (2010) 1717-1728.
[14] S.F. Badylak, D.J. Weiss, A. Caplan, P. Macchiarini, Engineered whole organs and complex tissues, Lancet 379 (2012) 943-952.
[15] K.S. Zaret, Hepatocyte differentiation: from the endoderm and beyond, Curr Opin Genet Dev 11 (2001) 568-574.

[16] P. Gripon, S. Rumin, S. Urban, J. Le Seyec, D. Glaise, I. Cannie, C. Guyomard, J. Lucas, C. Trepo, C. Guguen-Guillouzo, Infection of a human hepatoma cell line by hepatitis B virus, Proc Natl Acad Sci U S A 99 (2002) 15655-15660.
[17] C. Aninat, A. Piton, D. Glaise, T. Le Charpentier, S. Langouet, F. Morel, C. Guguen-Guillouzo, A. Guillouzo, Expression of cytochromes P450, conjugating enzymes and nuclear receptors in human hepatoma HepaRG cells, Drug Metab Dispos 34 (2006) 75-83.
[18] V. Cerec, D. Glaise, D. Garnier, S. Morosan, B. Turlin, B. Drenou, P. Gripon, D. Kremsdorf, C. Guguen-Guillouzo, A. Corlu, Transdifferentiation of hepatocyte-like cells from the human hepatoma HepaRG cell line through bipotent progenitor, Hepatology 45 (2007) 957-967.
[19] H. Herrema, D. Czajkowska, D. Theard, J.M. van der Wouden, D. Kalicharan, B. Zolghadr, D. Hoekstra, S.C. van Ijzendoorn, Rho kinase, myosin-II, and p42/44 MAPK control extracellular matrix-mediated apical bile canalicular lumen morphogenesis in HepG2 cells, Mol Biol Cell 17 (2006) 3291-3303.
[20] Y.R. Lou, L. Kanninen, T. Kuisma, J. Niklander, L.A. Noon, D. Burks, A. Urtti, M. Yliperttula, The use of nanofibrillar cellulose hydrogel as a flexible three-dimensional model to culture human pluripotent stem cells, Stem Cells Dev 23 (2014) 380-392.
[21] K.A. D'Amour, A.D. Agulnick, S. Eliazer, O.G. Kelly, E. Kroon, E.E. Baetge, Efficient differentiation of human embryonic stem cells to definitive endoderm, Nat Biotechnol 23 (2005) 1534-1541.
[22] D.C. Hay, J. Fletcher, C. Payne, J.D. Terrace, R.C. Gallagher, J. Snoeys, J.R. Black, D. Wojtacha, K. Samuel, Z. Hannoun, A. Pryde, C. Filippi, I.S. Currie, S.J. Forbes, J.A. Ross, P.N. Newsome, J.P. Iredale, Highly efficient differentiation of hESCs to functional hepatic endoderm requires ActivinA and Wnt3a signaling, Proc Natl Acad Sci U S A 105 (2008) 12301-12306.
[23] M.W. Pfaffl, A new mathematical model for relative quantification in real-time RT-PCR, Nucleic Acids Res 29 (2001) e45.
[24] S. Toivonen, K. Lundin, D. Balboa, J. Ustinov, K. Tamminen, J. Palgi, R. Trokovic, T. Tuuri, T. Otonkoski, Activin A and Wnt-dependent specification of human definitive endoderm cells, Exp Cell Res 319 (2013) 2535-2544.
[25] D.C. Hay, D. Zhao, A. Ross, R. Mandalam, J. Lebkowski, W. Cui, Direct differentiation of human embryonic stem cells to hepatocyte-like cells exhibiting functional activities, Cloning Stem Cells 9 (2007) 51-62.
[26] Y. Kono, S. Yang, E.A. Roberts, Extended primary culture of human hepatocytes in a collagen gel sandwich system, In Vitro Cell Dev Biol Anim 33 (1997) 467-472.
[27] G.A. Hamilton, S.L. Jolley, D. Gilbert, D.J. Coon, S. Barros, E.L. LeCluyse, Regulation of cell morphology and cytochrome P450 expression in human hepatocytes by extracellular matrix and cell-cell interactions, Cell Tissue Res 306 (2001) 85-99.
[28] N. Katsura, I. Ikai, T. Mitaka, T. Shiotani, S. Yamanokuchi, S. Sugimoto, A. Kanazawa, H. Terajima, Y. Mochizuki, Y. Yamaoka, Long-term culture of primary human hepatocytes with preservation of proliferative capacity and differentiated functions, J Surg Res 106 (2002) 115-123.
[29] C.S. Lee, J.R. Friedman, J.T. Fulmer, K.H. Kaestner, The initiation of liver development is dependent on Foxa transcription factors, Nature 435 (2005) 944-947.
[30] E. Schmelzer, L. Zhang, A. Bruce, E. Wauthier, J. Ludlow, H.L. Yao, N. Moss, A. Melhem, R. McClelland, W. Turner, M. Kulik, S. Sherwood, T. Tallheden, N. Cheng, M.E. Furth, L.M. Reid, Human hepatic stem cells from fetal and postnatal donors, J Exp Med 204 (2007) 1973-1987.
[31] W.P. Daley, S.B. Peters, M. Larsen, Extracellular matrix dynamics in development and regenerative medicine, J Cell Sci 121 (2008) 255-264.
[32] P. Lu, K. Takai, V.M. Weaver, Z. Werb, Extracellular matrix degradation and remodeling in development and disease, Cold Spring Harb Perspect Biol 3 (2011).
[33] D.A. Brafman, C. Phung, N. Kumar, K. Willert, Regulation of endodermal differentiation of human embryonic stem cells through integrin-ECM interactions, Cell Death Differ 20 (2013) 369-381.
[34] J.C. Wong, S.Y. Gao, J.G. Lees, M.B. Best, R. Wang, B.E. Tuch, Definitive endoderm derived from human embryonic stem cells highly express the integrin receptors alphaV and beta5, Cell Adh Migr 4 (2010) 39-45.
[35] J.D. Humphries, A. Byron, M.J. Humphries, Integrin ligands at a glance, J Cell Sci 119 (2006) 3901-3903.

[36] Y. Wang, C.B. Cui, M. Yamauchi, P. Miguez, M. Roach, R. Malavarca, M.J. Costello, V. Cardinale, E. Wauthier, C. Barbier, D.A. Gerber, D. Alvaro, L.M. Reid, Lineage restriction of human hepatic stem cells to mature fates is made efficient by tissue-specific biomatrix scaffolds, Hepatology 53 (2011) 293-305.
[37] R. Lang, M.M. Stern, L. Smith, Y. Liu, S. Bharadwaj, G. Liu, P.M. Baptista, C.R. Bergman, S. Soker, J.J. Yoo, A. Atala, Y. Zhang, Three-dimensional culture of hepatocytes on porcine liver tissue-derived extracellular matrix, Biomaterials 32 (2011) 7042-7052.
[38] B.E. Uygun, A. Soto-Gutierrez, H. Yagi, M.L. Izamis, M.A. Guzzardi, C. Shulman, J. Milwid, N. Kobayashi, A. Tilles, F. Berthiaume, M. Hertl, Y. Nahmias, M.L. Yarmush, K. Uygun, Organ reengineering through development of a transplantable recellularized liver graft using decellularized liver matrix, Nat Med 16 (2010) 814-820.
[39] Y. Higuchi, N. Shiraki, K. Yamane, Z. Qin, K. Mochitate, K. Araki, T. Senokuchi, K. Yamagata, M. Hara, K. Kume, S. Kume, Synthesized basement membranes direct the differentiation of mouse embryonic stem cells into pancreatic lineages, J Cell Sci 123 (2010) 2733-2742.
[40] T. Hoshiba, N. Kawazoe, T. Tateishi, G. Chen, Development of stepwise osteogenesis-mimicking matrices for the regulation of mesenchymal stem cell functions, J Biol Chem 284 (2009) 31164-31173.
[41] T. Hoshiba, N. Kawazoe, T. Tateishi, G. Chen, Development of extracellular matrices mimicking stepwise adipogenesis of mesenchymal stem cells, Adv Mater 22 (2010) 3042-3047.
[42] K.H. Choi, B.H. Choi, S.R. Park, B.J. Kim, B.H. Min, The chondrogenic differentiation of mesenchymal stem cells on an extracellular matrix scaffold derived from porcine chondrocytes, Biomaterials 31 (2010) 5355-5365.
[43] C.P. Ng, A.R. Sharif, D.E. Heath, J.W. Chow, C.B. Zhang, M.B. Chan-Park, P.T. Hammond, J.K. Chan, L.G. Griffith, Enhanced ex vivo expansion of adult mesenchymal stem cells by fetal mesenchymal stem cell ECM, Biomaterials 35 (2014) 4046-4057.
[44] L.C. Boffa, G. Vidali, R.S. Mann, V.G. Allfrey, Suppression of histone deacetylation in vivo and in vitro by sodium butyrate, J Biol Chem 253 (1978) 3364-3366.
[45] J.E. Dyson, J. Daniel, C.R. Surrey, The effect of sodium butyrate on the growth characteristics of human cervix tumour cells, Br J Cancer 65 (1992) 803-808.
[46] T.S. Ramasamy, J.S. Yu, C. Selden, H. Hodgson, W. Cui, Application of three-dimensional culture conditions to human embryonic stem cell-derived definitive endoderm cells enhances hepatocyte differentiation and functionality, Tissue Eng Part A 19 (2013) 360-367.
[47] N.J. Sund, S.L. Ang, S.D. Sackett, W. Shen, N. Daigle, M.A. Magnuson, K.H. Kaestner, Hepatocyte nuclear factor 3beta (Foxa2) is dispensable for maintaining the differentiated state of the adult hepatocyte, Mol Cell Biol 20 (2000) 5175-5183.
[48] J. Li, G. Ning, S.A. Duncan, Mammalian hepatocyte differentiation requires the transcription factor HNF-4alpha, Genes Dev 14 (2000) 464-474.
[49] M. Kajiwara, T. Aoi, K. Okita, R. Takahashi, H. Inoue, N. Takayama, H. Endo, K. Eto, J. Toguchida, S. Uemoto, S. Yamanaka, Donor-dependent variations in hepatic differentiation from human-induced pluripotent stem cells, Proc Natl Acad Sci U S A 109 (2012) 12538-12543.
[50] M. Koyanagi-Aoi, M. Ohnuki, K. Takahashi, K. Okita, H. Noma, Y. Sawamura, I. Teramoto, M. Narita, Y. Sato, T. Ichisaka, N. Amano, A. Watanabe, A. Morizane, Y. Yamada, T. Sato, J. Takahashi, S. Yamanaka, Differentiation-defective phenotypes revealed by large-scale analyses of human pluripotent stem cells, Proc Natl Acad Sci U S A 110 (2013) 20569-20574.
[51] Z. Li, S. Hu, Z. Ghosh, Z. Han, J.C. Wu, Functional characterization and expression profiling of human induced pluripotent stem cell- and embryonic stem cell-derived endothelial cells, Stem Cells Dev 20 (2011) 1701-1710.
[52] S. Ogawa, J. Surapisitchat, C. Virtanen, M. Ogawa, M. Niapour, K.S. Sugamori, S. Wang, L. Tamblyn, C. Guillemette, E. Hoffmann, B. Zhao, S. Strom, R.R. Laposa, R.F. Tyndale, D.M. Grant, G. Keller, Three-dimensional culture and cAMP signaling promote the maturation of human pluripotent stem cell-derived hepatocytes, Development 140 (2013) 3285-3296.
[53] G.D. Block, J. Locker, W.C. Bowen, B.E. Petersen, S. Katyal, S.C. Strom, T. Riley, T.A. Howard, G.K. Michalopoulos, Population expansion, clonal growth, and specific differentiation patterns in primary cultures of hepatocytes induced by HGF/SF, EGF and TGF alpha in a chemically defined (HGM) medium, J Cell Biol 132 (1996) 1133-1149.

[54] P.B. Limaye, W.C. Bowen, A.V. Orr, J. Luo, G.C. Tseng, G.K. Michalopoulos, Mechanisms of hepatocyte growth factor-mediated and epidermal growth factor-mediated signaling in transdifferentiation of rat hepatocytes to biliary epithelium, Hepatology 47 (2008) 1702-1713.
[55] J.C. Dunn, M.L. Yarmush, H.G. Koebe, R.G. Tompkins, Hepatocyte function and extracellular matrix geometry: long-term culture in a sandwich configuration, FASEB J 3 (1989) 174-177.
[56] A.T. Gutsche, H. Lo, J. Zurlo, J. Yager, K.W. Leong, Engineering of a sugar-derivatized porous network for hepatocyte culture, Biomaterials 17 (1996) 387-393.
[57] S.M. Chia, K.W. Leong, J. Li, X. Xu, K. Zeng, P.N. Er, S. Gao, H. Yu, Hepatocyte encapsulation for enhanced cellular functions, Tissue Eng 6 (2000) 481-495.
[58] C. Yin, S. Mien Chia, C. Hoon Quek, H. Yu, R.X. Zhuo, K.W. Leong, H.Q. Mao, Microcapsules with improved mechanical stability for hepatocyte culture, Biomaterials 24 (2003) 1771-1780.

A

Supplement to RPMI-1640 medium	M1	M2	M3	M4
1 x GlutaMAX (Gibco, 35050-061)	x	x	x	x
1 x B-27 (Gibco, 17504-044)	x	x	x	x
100 ng/ml Activin A (PeproTech, 120-14E)	x	x		
100 ng/ml Activin A (Gibco, PHG9014)			x	x
75 ng/ml Wnt-3a (R&D Systems, 5036-WN-010/CF)	x		x	
1 mM (day 0) and 0.5 mM (days 1-5) Sodium butyrate (Sigma-Aldrich, B5887)	x		x	

B

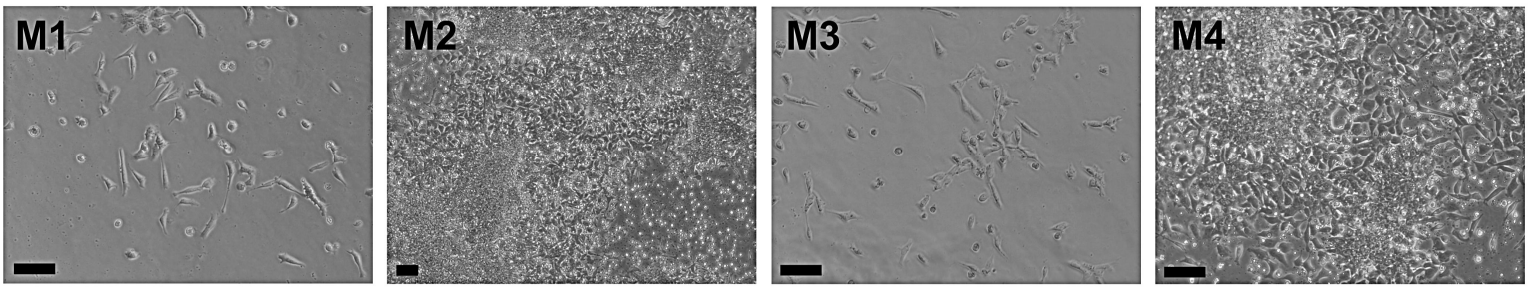

C

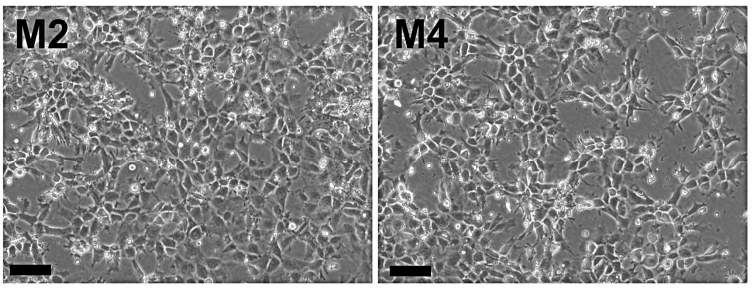

D

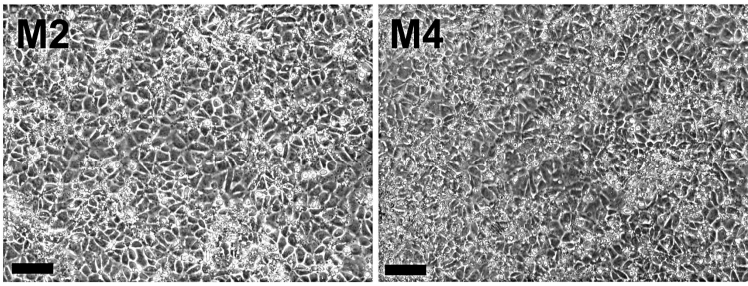

E

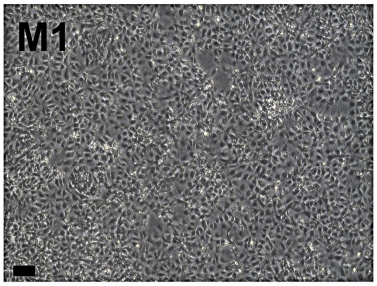

F

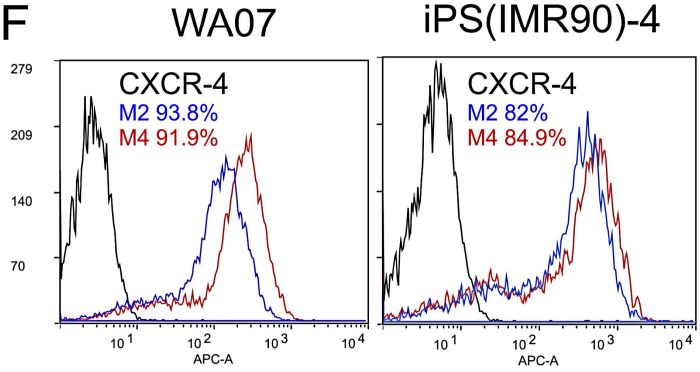

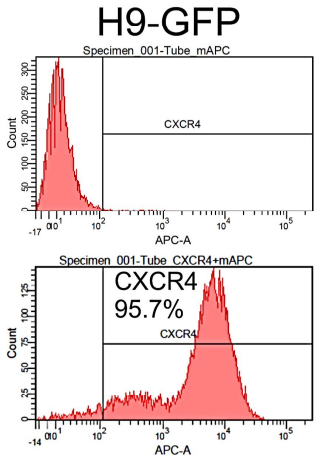

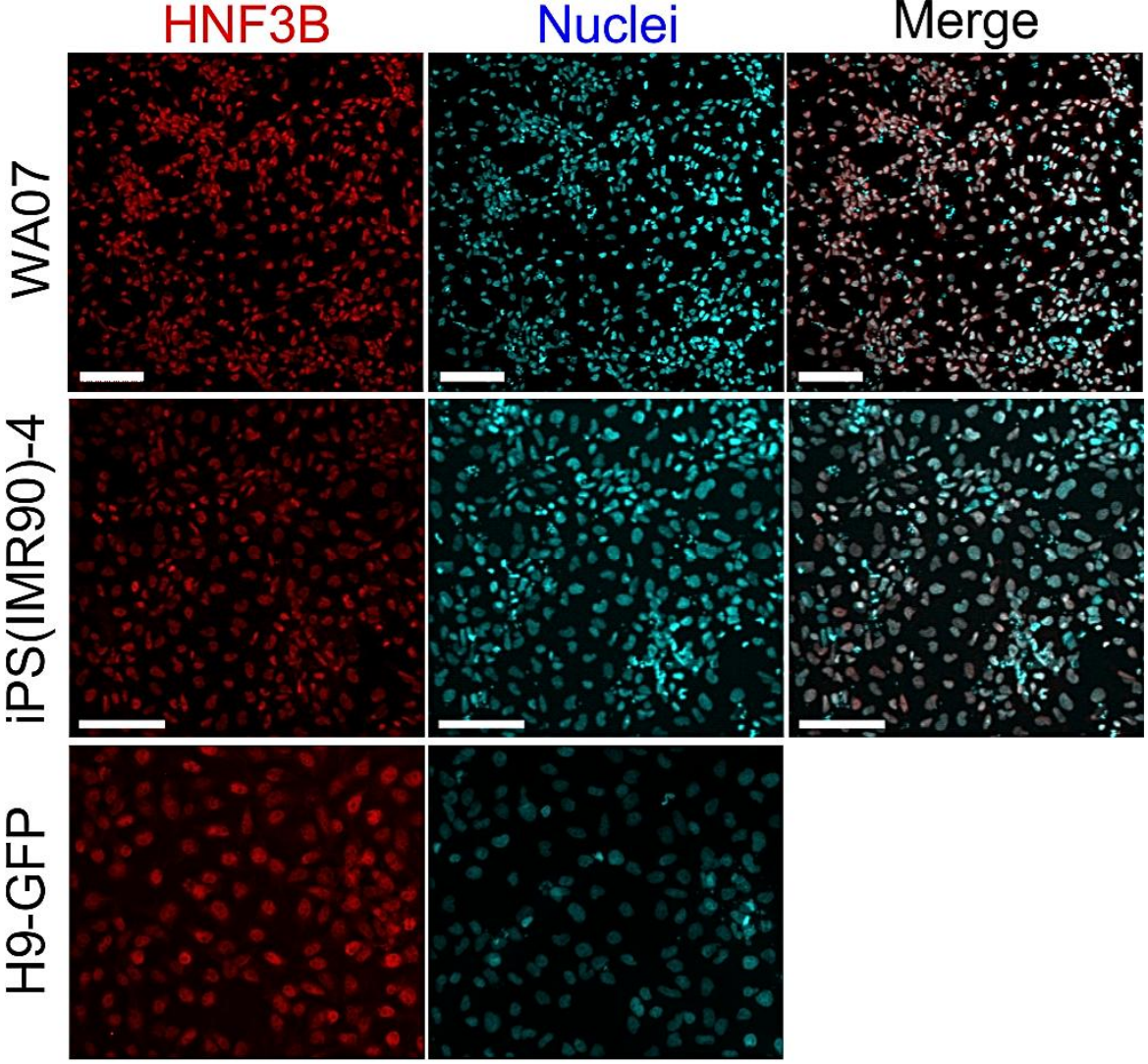
HNF3B
Nuclei
Merge
WA07
iPS(IMR90)-4
H9-GFP

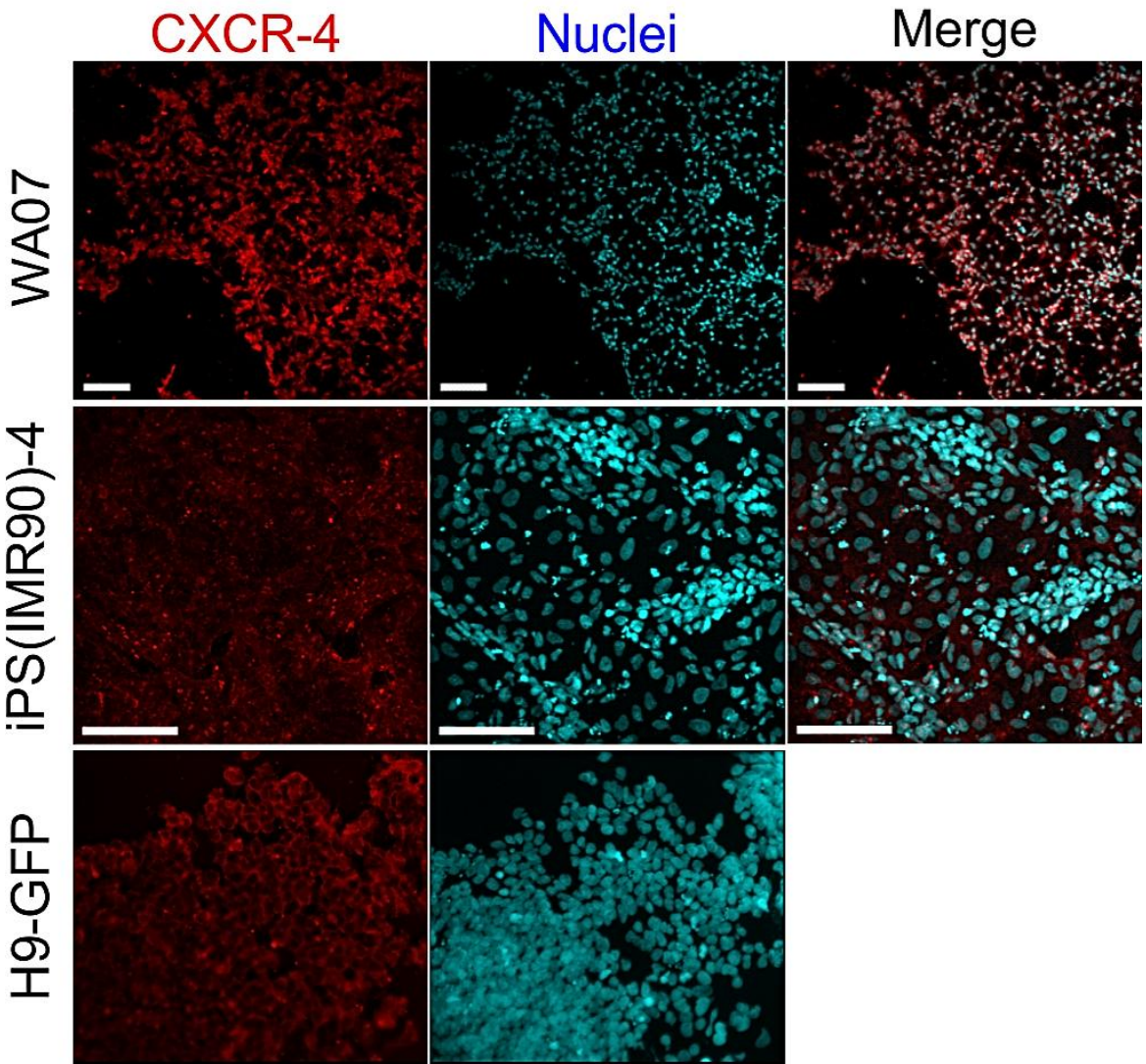
CXCR-4
Nuclei
Merge
WA07
iPS(IMR90)-4
H9-GFP

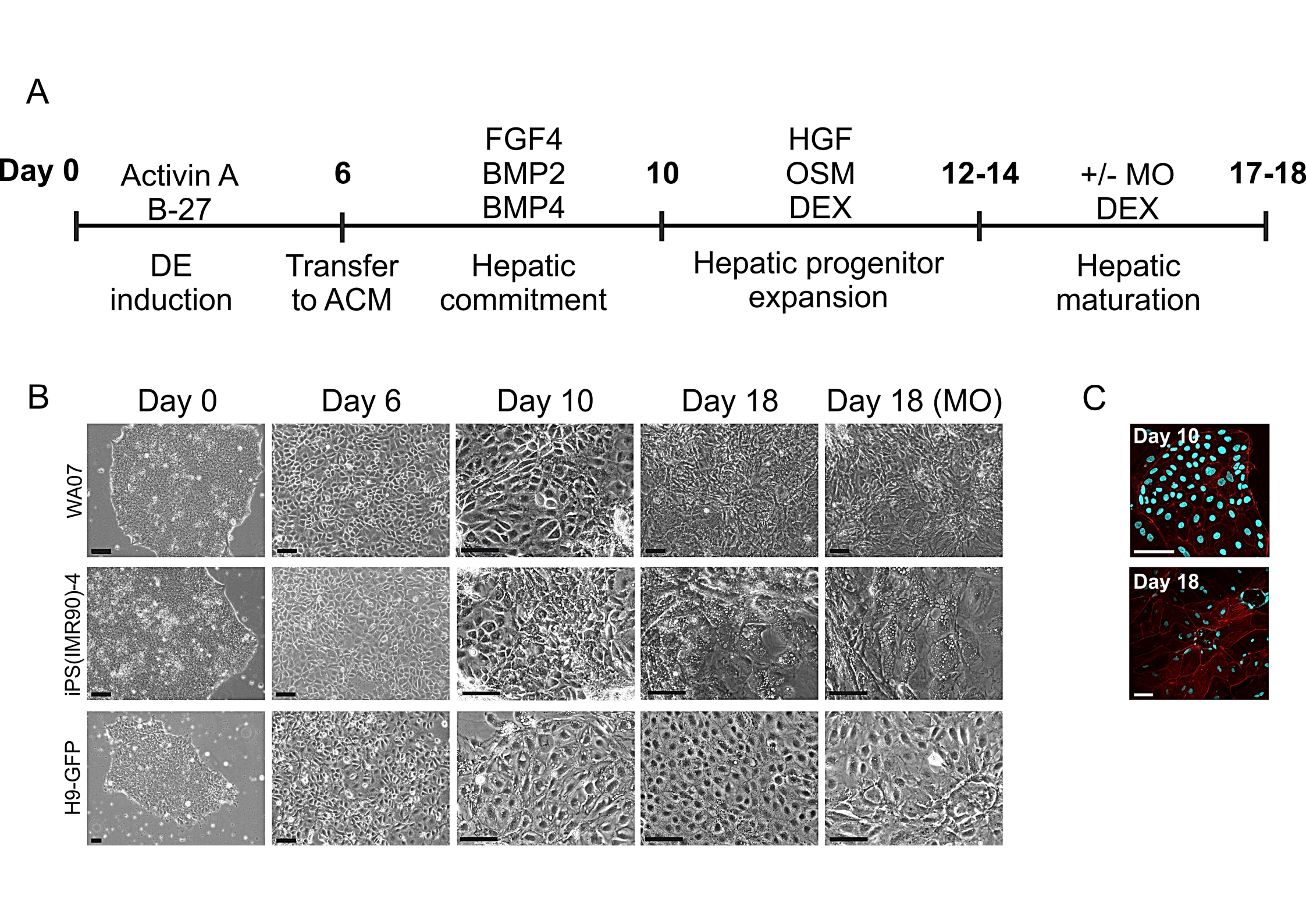
A
Day 0
Activin A
B-27
6
FGF4
BMP2
BMP4
10
HGF
OSM
DEX
12-14
+/- MO
DEX
17-18
DE
induction
Transfer
to ACM
Hepatic
commitment
Hepatic progenitor
expansion
Hepatic
maturation
B
Day 0
Day 6
Day 10
Day 18
Day 18 (MO)
WA07
iPS(IMR90)-4
H9-GFP
C
Day 10
Day 18

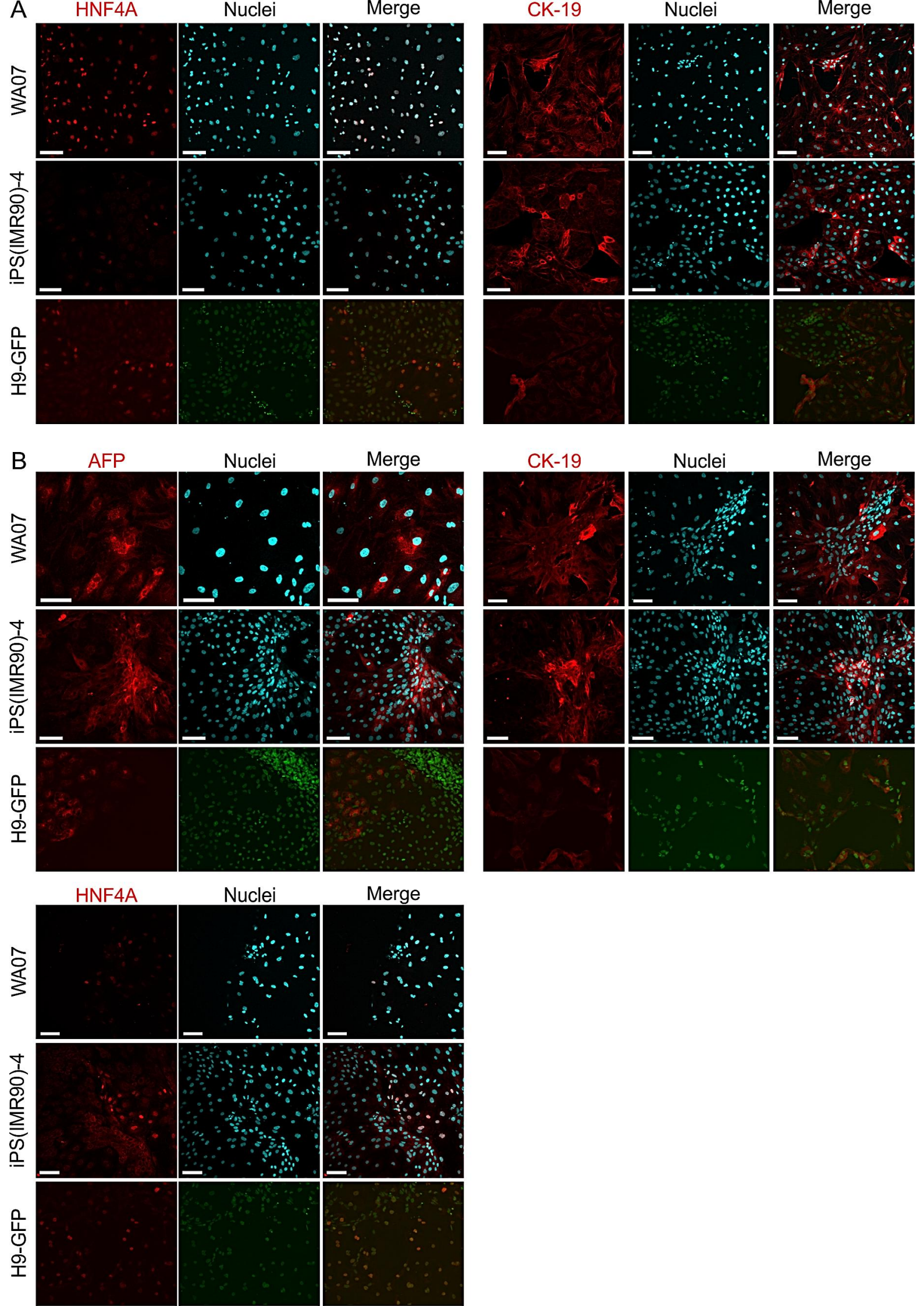
A
HNF4A
Nuclei
Merge
CK-19
Nuclei
Merge
WA07
iPS(IMR90)-4
H9-GFP
B
AFP
Nuclei
Merge
CK-19
Nuclei
Merge
WA07
iPS(IMR90)-4
H9-GFP
HNF4A
Nuclei
Merge
WA07
iPS(IMR90)-4
H9-GFP

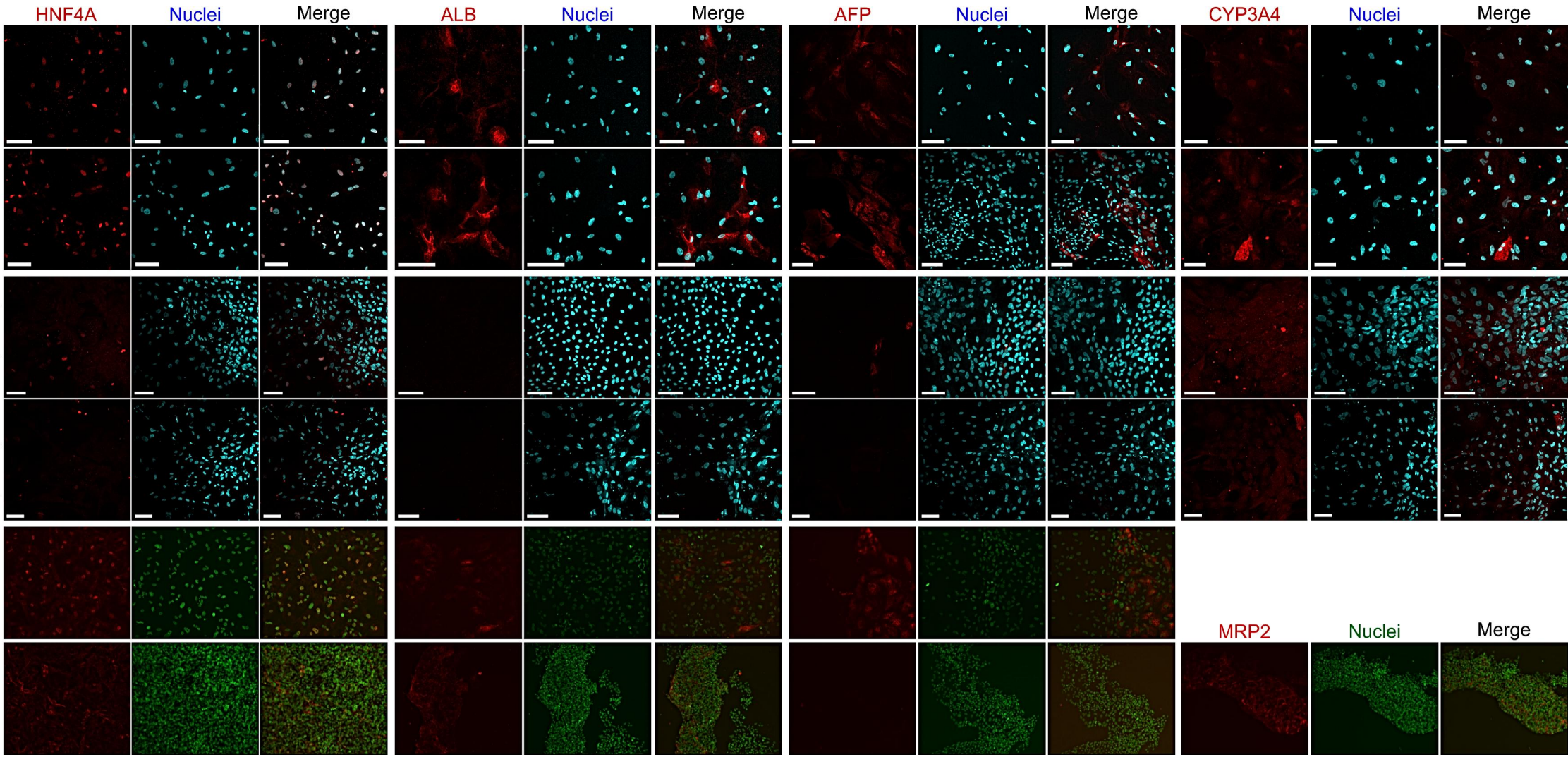
HNF4A
Nuclei
Merge
ALB
Nuclei
Merge
AFP
Nuclei
Merge
CYP3A4
Nuclei
Merge
WA07
WA07 MO
iPS(IMR90)-4
iPS(IMR90)-4 MO
H9-GFP
H9-GFP MO
MRP2
Nuclei
Merge

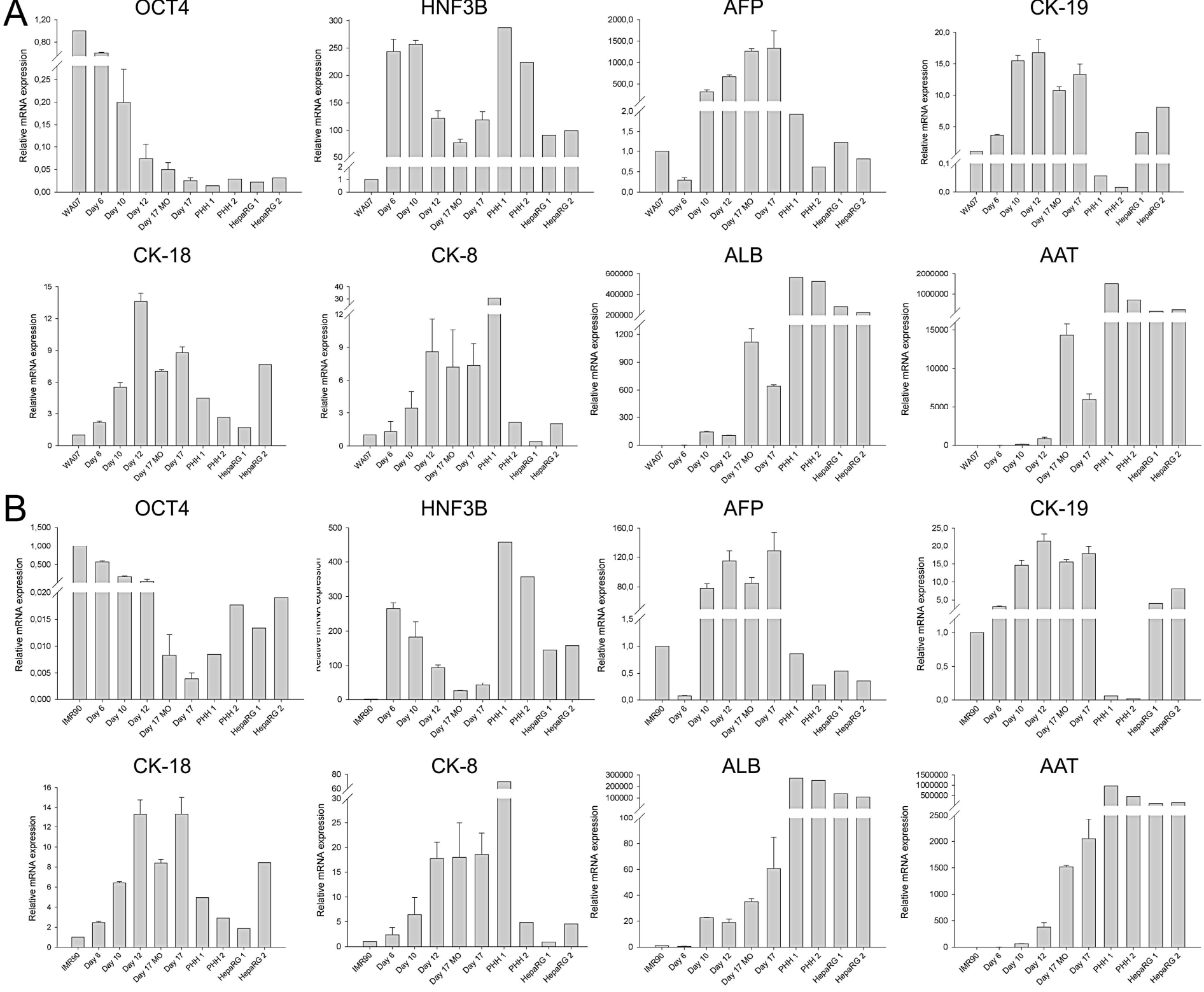
A
OCT4
HNF3B
AFP
CK-19
CK-18
CK-8
ALB
AAT
B
OCT4
HNF3B
AFP
CK-19
CK-18
CK-8
ALB
AAT
Relative mRNA expression
WA07
IMR90
Day 6
Day 10
Day 12
Day 17 MO
Day 17
PHH 1
PHH 2
HepaRG 1
HepaRG 2

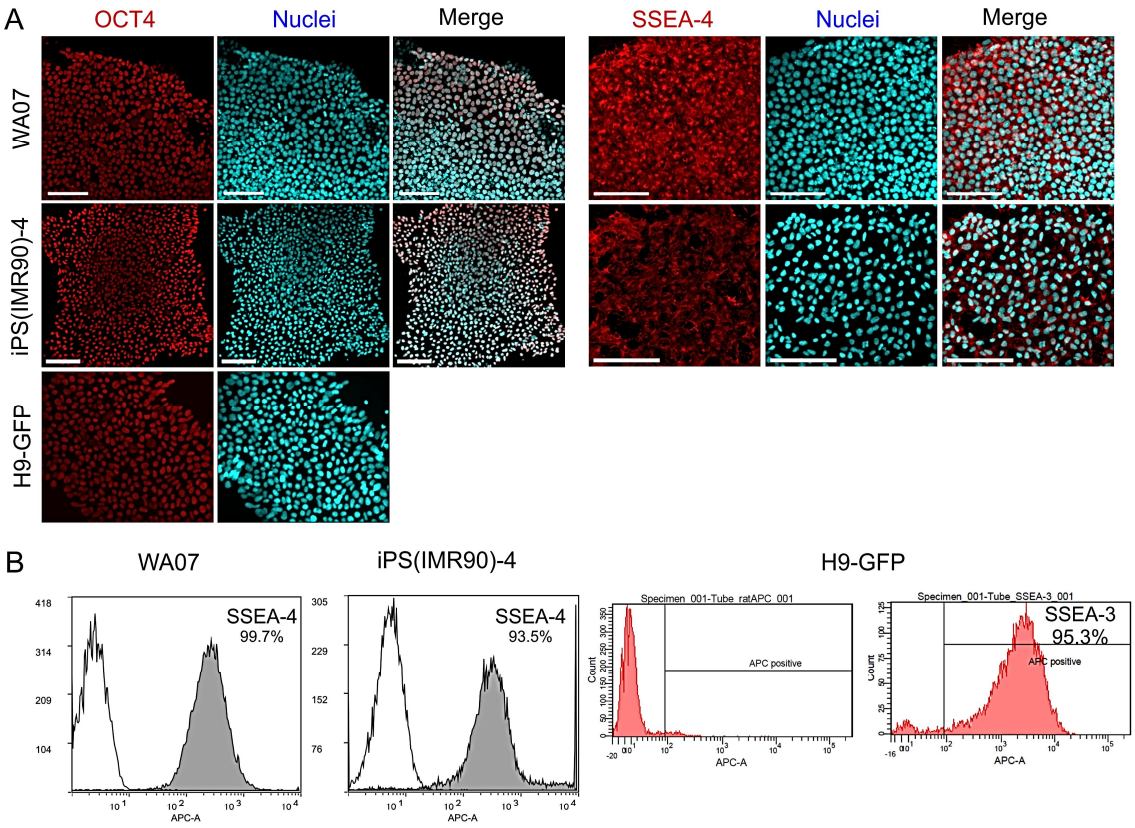

Fig. S1. Characterization of the WA07, iPS(IMR90)-4, and H9-GFP cells. (A) Immunofluorescence of the pluripotency markers *OCT4* and *SSEA-4* in the hPSCs. Scale bars = 100 µm. 20x magnification for the H9-GFP cells. (B) Flow cytometry analyses of the *SSEA-4* expression in the WA07 and iPS(IMR90)-4 cells and *SSEA-3* expression in the H9-GFP cells.

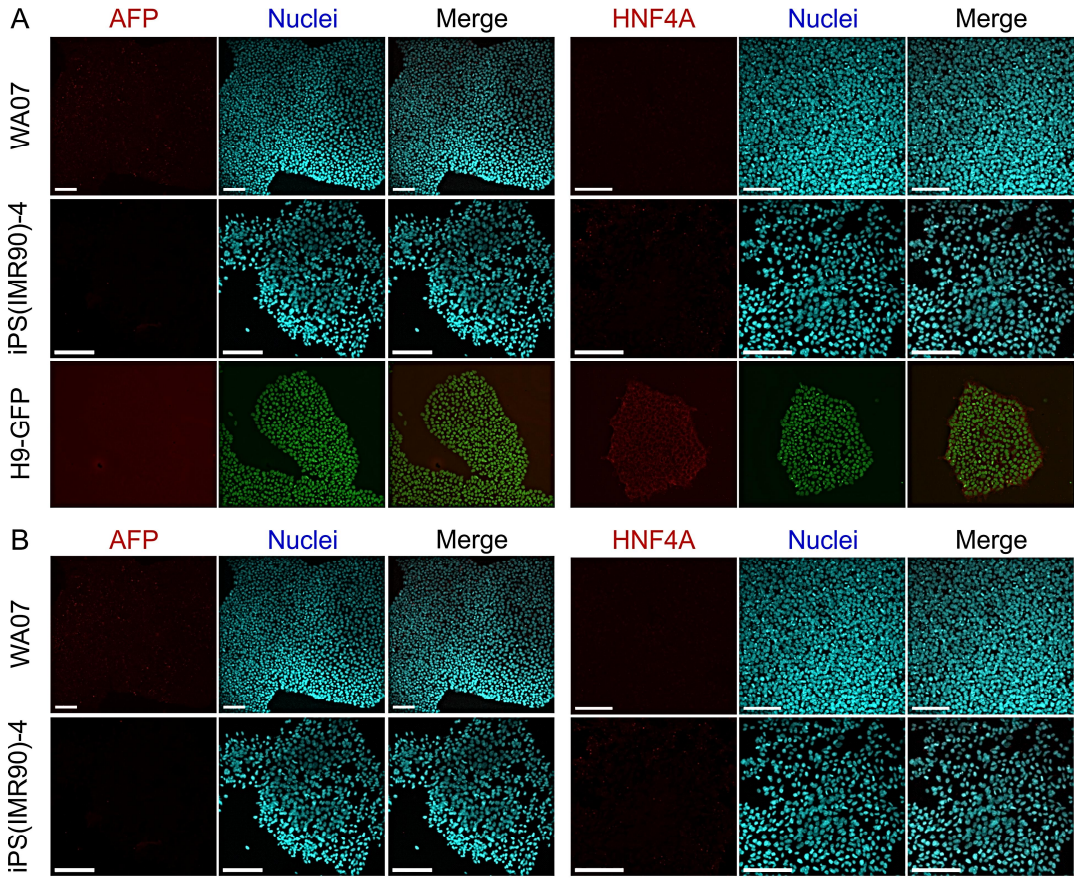

Fig. S2. The protein expression of hepatic markers *AFP* and *HNF4A*. (A) the WA07, iPS(IMR90)-4, and H9-GFP cells. (B) the hPSC-derived DE cells. Scale bars = 100 μm; 10x magnification for the II9-GFP cells.

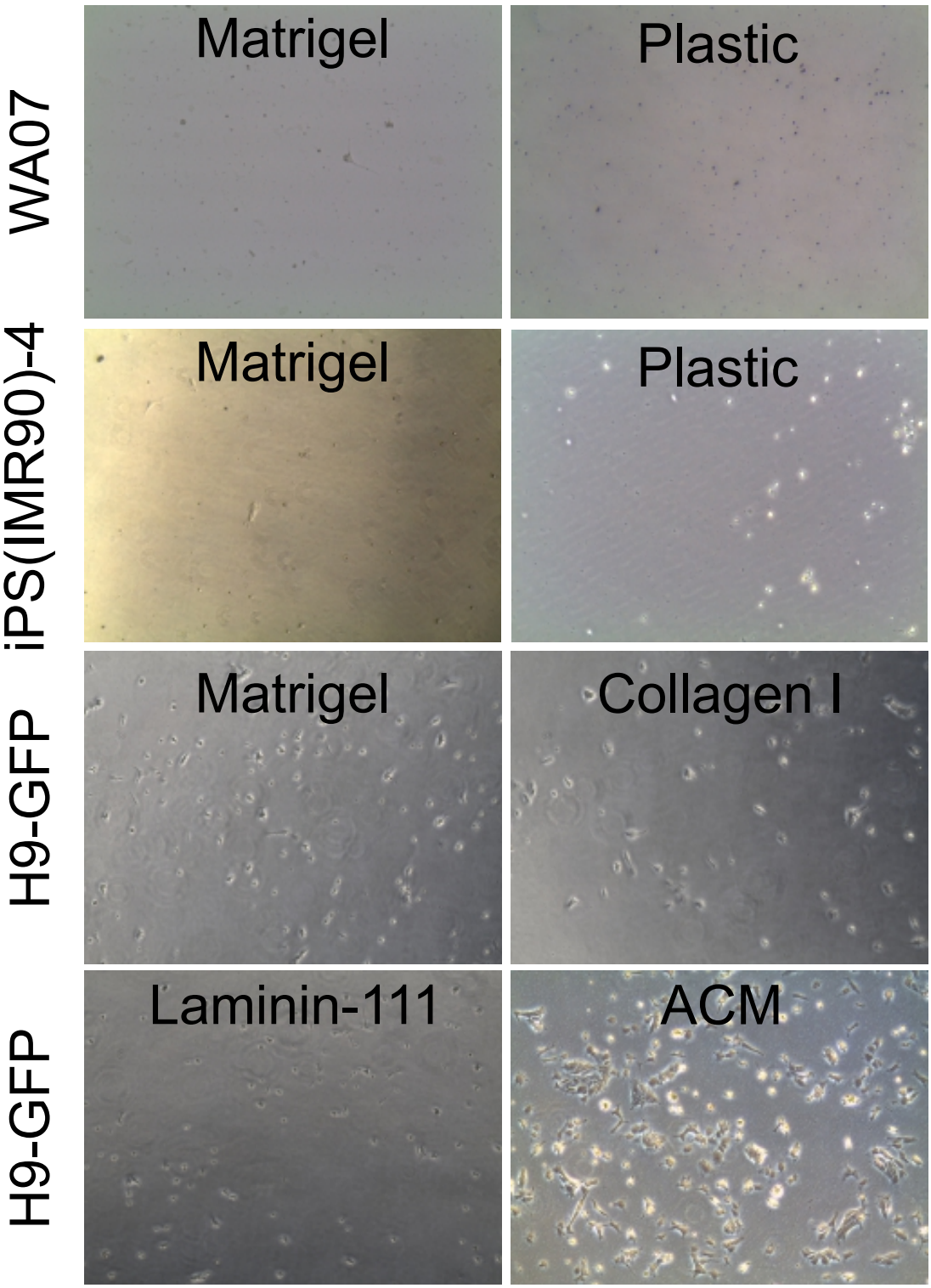

Fig. S3. DE cell attachment on different coatings one day (iPS(IMR90)-4 and H9-GFP) or two days (WA07) after cell seeding. 5x magnification.

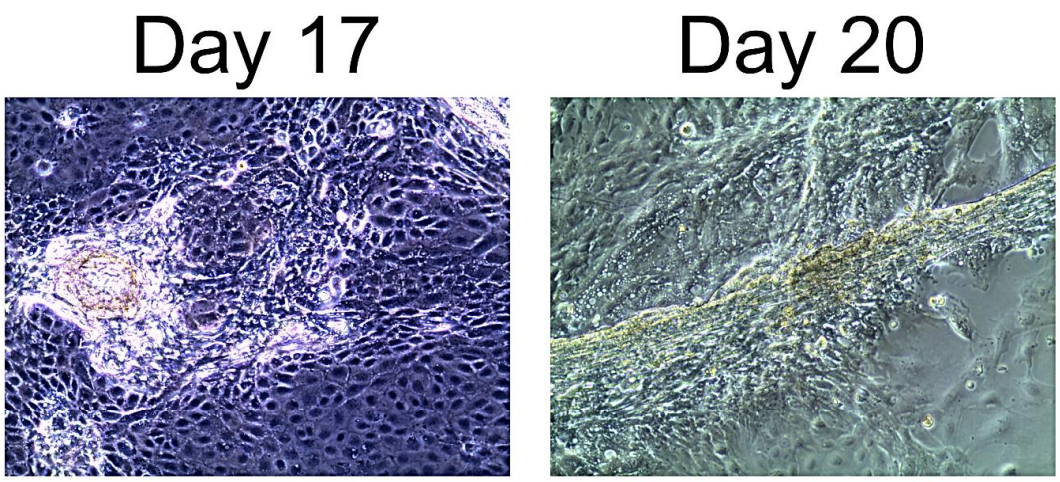

Fig. S4. Formation of ductular structures during hepatic maturation of H9-GFP cells in the presence of HGF. 10x magnification.

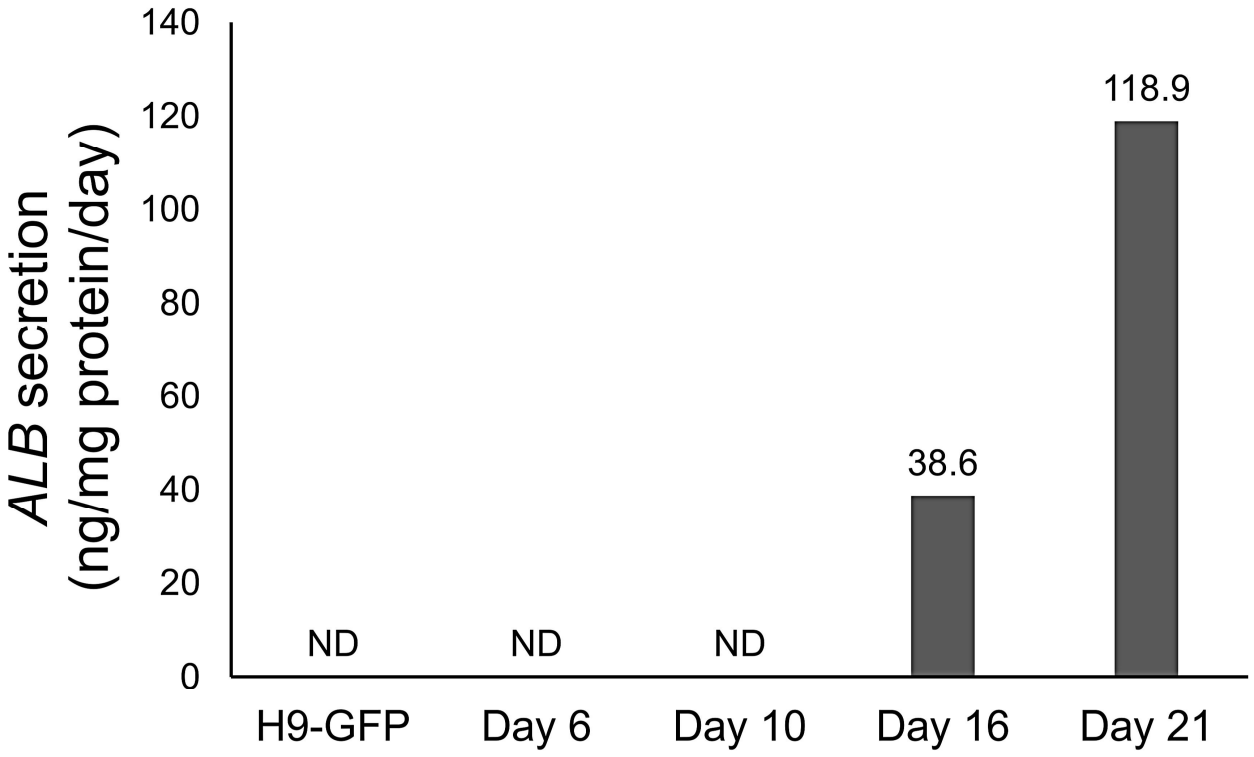

Fig. S5. *ALB* secretion by the H9-GFP cells during the differentiation.

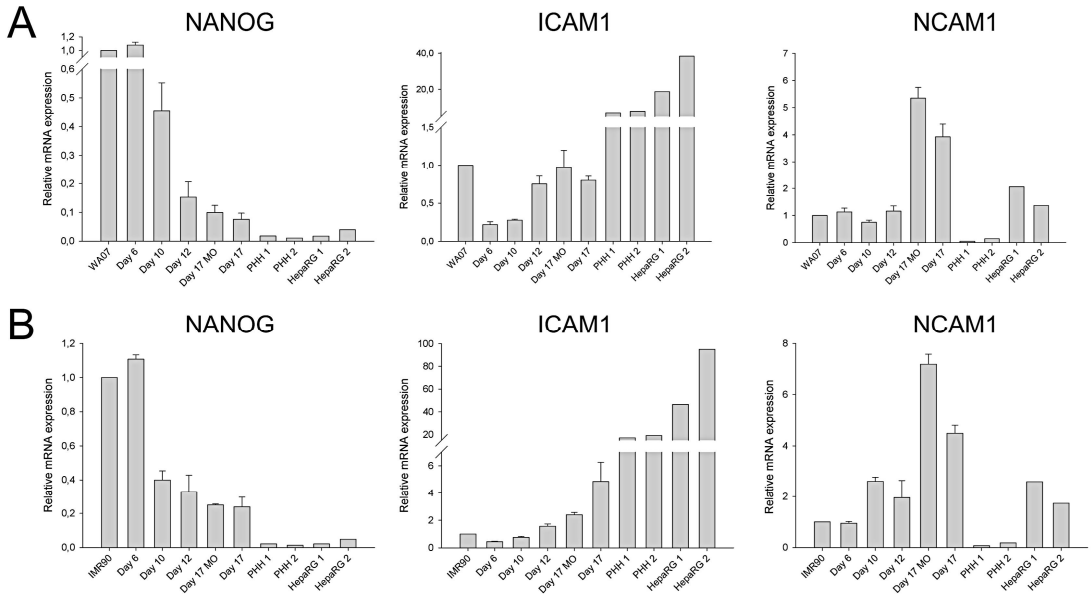

Fig. S6. Relative mRNA expression of the pluripotency and liver markers in the WA07 and iPS(IMR90)-4 cells during the differentiation. The mRNA expression of *NANOG*, *ICAM1*, and *NCAM1* in the WA07 (A) and iPS(IMR90)-4 (B) cells during the differentiation was analyzed by real-time qPCR. Relative mRNA expression was normalized to the control gene *RPLP0*, and fold inductions were calculated with reference to the undifferentiated WA07 or iPS(IMR90)-4 cells on day 0. N = 3 biological samples. Error bars are SD. MO = Matrigel overlay; PHH 1: primary human hepatocytes (BD Biosciences, 454503, lot HH177); PHH 2: primary human hepatocytes (BD Biosciences, 454503, lot 99); HepaRG 1: two-week culture without DMSO treatment; HepaRG 2: two-week culture without DMSO treatment followed by two week differentiation in 2% DMSO.

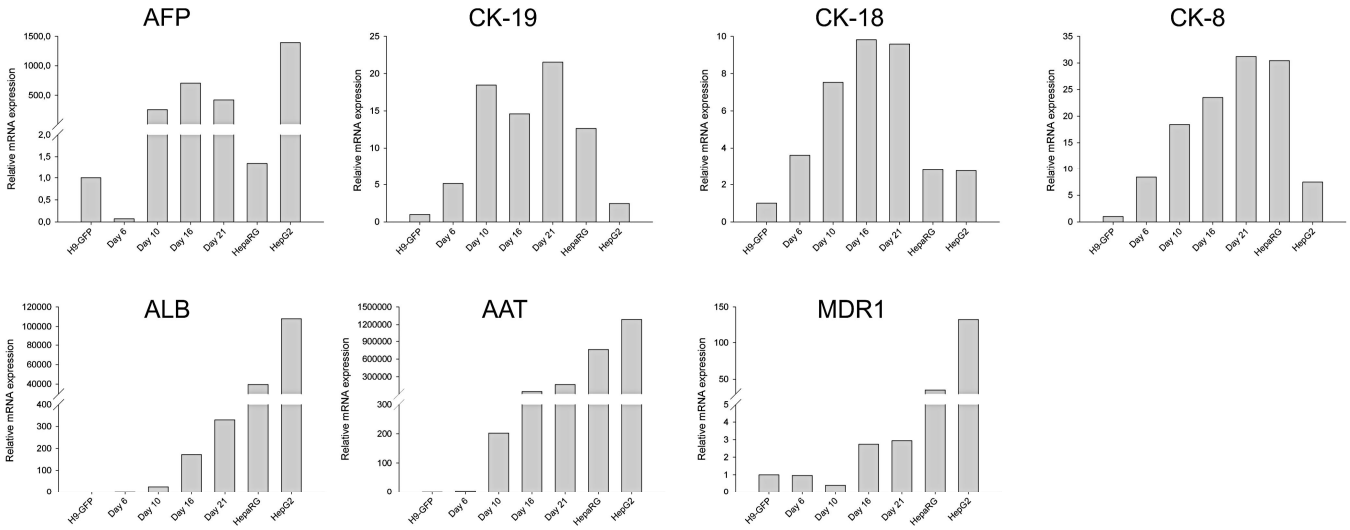

Fig. S7. Relative mRNA expression of the liver markers in the H9-GFP cells during the differentiation. The mRNA expression of *AFP*, *CK-19*, *CK-18*, *CK-8*, *ALB*, *AAT*, and *MDR1* in the H9-GFP cells during the differentiation was analyzed by real-time qPCR. Relative mRNA expression was normalized to the control gene *RPLP0*, and fold inductions were calculated with reference to the undifferentiated H9-GFP cells on day 0. HepaRG: two-week culture without DMSO treatment.

Table S1

Antibodies used in immunofluorescence.

Antigen	**Antibody manufacturer**	**Antibody catalog number**	**Antibody dilution**
Alpha fetoprotein (*AFP*)	Sigma-Aldrich	A8452	1:500
Albumin (*ALB*)	Bethyl Laboratories	A80-229A	1:500
Cytokeratin 19 (*CK-19*, also known as *KRT19*)	Santa Cruz Biotechnology	sc-6287	1:50
CXCR-4	R&D Systems	MAB172	1:50
Cytochrome P450 3A4 (*CYP3A4*)	Millipore	AB1254	1:500
Hepatocyte nuclear factor 3B (*HNF3B*, also known as *FOXA2*)	Santa Cruz Biotechnology	sc-6554	1:50
HNF4A	Santa Cruz Biotechnology	sc-6556	1:200
ATP-binding cassette, sub-family C, member 2 (*MRP2*, also known as *ABCC2*)	abcam	ab3373	1:50
Octamer-binding transcription factor 4 (*OCT4*)	Santa Cruz Biotechnology	sc-9081	1:500
SSEA-4	Developmental Studies Hybridoma Bank	MC-813-70	1:100

Table S2

Primers used in real-time qPCR.

Gene	Accession	Size (bp)	Sequence (5’ to 3’)
RPLP0	NM_001002.3 NM_053275.3	74	F: AATCTCCAGGGGCACCATT R: CGCTGGCTCCCACTTTGT
OCT4	NM_002701.4 NM_203289.4 NM_001173531.1	161	F: CAGTGCCCGAAACCCACAC R: GGAGACCCAGCAGCCTCAAA
NANOG	NM_024865.2	80	F: GCAGAAGGCCTCAGCACCTA R: GGTTCCCAGTCGGGTTCAC
HNF3B (*FOXA2*)	NM_021784.4 NM_153675.2	89	F: GGGAGCGGTGAAGATGGA R: TCATGTTGCTCACGGAGGAGTA
AFP	NM_001134.1	79	F: GTTGCCAACTCAGTGAGGACAA R: CTGATACATAAGTGTCCGATAATAATGTCA
CK-8	NM_002273.2	134	F: TCTCTGAGATGAACCGGAACAT R: GGCGTTGGCATCCTTAATG
CK-18	NM_199187.1 NM_000224.2	70	F: ATGGCGAGGACTTTAATCTTGGT R: GTGGTCTTTTGGATGGTTTGC
CK-19	NM_002276.4	142	F: AGCATGAAAGCTGCCTTGGA R: CCTGATTCTGCCGCTCACTATC
ALB	NM_000477.3	85	F: AAGTGGGCAGCAAATGTTGTAA R: AACTGGTTCAGGACCACGGATA
AAT	NM_000295.3	135	F: GGCCAAGAAACAGATCAACGAT R: GGTCTCTCCCATTTGCCTTTAA
ICAM1	NM_000201.2	107	F: TGAGCAATGTGCAAGAAGATAGC R: CACCCGTTCTGGAGTCCAGTAC
NCAM1	NM_000615.5	144	F: GGTGCCCATCCTCAAATACAAA R: CTTACGGCGTACGTTGTTTCG
MDR1	NM_000927.4	202	F: GCTCCTGACTATGCCAAAGC R: TCTTCACCTCCAGGCTCAGT

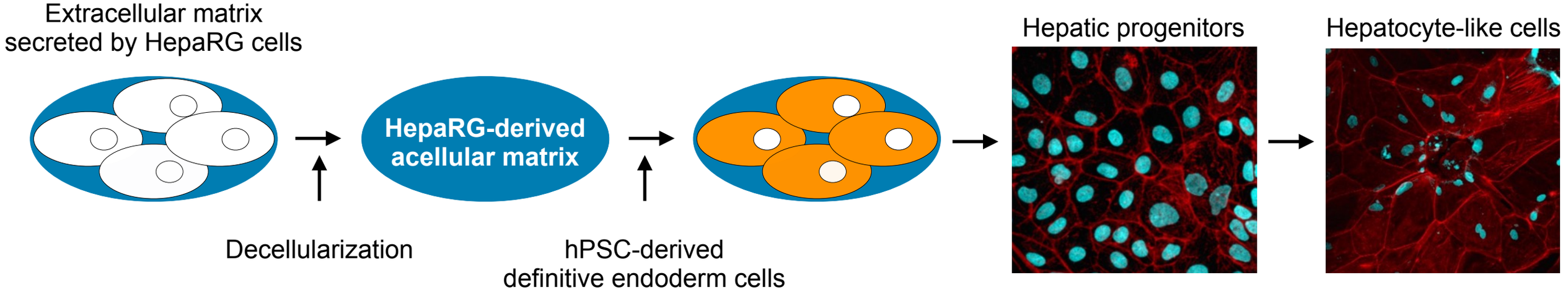
Extracellular matrix
secreted by HepaRG cells
HepaRG-derived
acellular matrix
Decellularization
hPSC-derived
definitive endoderm cells
Hepatic progenitors
Hepatocyte-like cells

Highlights

- We first report HepaRG acellular matrix (ACM) promotes hepatic commitment of hPSCs.
- Definitive endoderm cells attached and differentiated to hepatic cells on HepaRG ACM.
- Matrigel overlay improved hepatic maturation.
- We report the importance of the matrix in hepatic differentiation.